

UNIVERSITÀ
DEGLI STUDI
DI PADOVA

UNIVERSITA' DEGLI STUDI DI PADOVA

Dipartimento di Ingegneria Industriale DII

Corso di Laurea Magistrale in Ingegneria dei Materiali

Multi-physical analysis of the buckling behaviour of a metal strip in a
transverse flux induction heating process

Prof. Fabrizio Dughiero
Prof. Egbert Baake
Dr. Alexander Nikanorov

Francesco Beghin
N° matricola: 1179189

Anno Accademico 2019/2020

Abstract

The focus of this work is the study of the buckling behaviour of a metal strip in a transverse flux induction heating process. In particular, a FEM model was developed in order to simulate the aforementioned process. The thesis will present the step by step construction of the code. The model consists of a Multiphysics simulation: thermal and structural. The structural part is a combination of the ANSYS® buckling analyses: *Eigenvalue linear buckling analysis* and *non-linear buckling analysis*. As it was not possible to get an experimental validation of the results, the work focused on the parametrical analysis of the developed model. The purpose was to check the consistency as well as the physical accuracy of the results.

The parametrical analysis dealt with the variation of several parameters, such as: strip length, applied forces, mechanical constraints, material properties, temperature field and strip thickness.

In the end, the model proved to be a useful tool for the analysis of thermal buckling, particularly, in the frame of induction heating processes. This work could represent a small piece of a 360 degrees Multiphysics analysis of such processes.

Table of contents

Abstract	2
Acknowledgements	5
Introduction	6
<i>Structure of the thesis</i>	7
1 Preliminary notions	8
1.1 Induction heating principles	8
1.2 Induction heating processes	9
1.3 Strip deformation in TFH	12
1.4 Applications of TFH - Example	14
1.5 Buckling Phenomenon	14
2 The FEM Simulation	16
2.1 Multiphysics simulations	16
2.2 Buckling analysis in ANSYS Mechanical APDL®	17
2.2.1 The choice of the Element Type in the FEM analysis.....	18
2.2.2 Solving Equations	19
3 The numerical model	22
3.1 General Description	22
3.2 Model Construction	23
3.2.1 Model Geometry	23
3.2.2 Attributes of the elements	26
3.3 Model boundary conditions	29
3.3.1 Thermal environment	29
3.3.2 Structural environment.....	33
3.4 Model Meshing	35
3.4.1 Model validation through mesh variation.....	36
3.5 Main Settings: number of buckling modes and geometrical factor	37
4 Parametrical Analysis	40

4.1	<i>Length Parameter</i>	41
4.2	<i>Applied Force Parameter</i>	43
4.3	<i>Mechanical Constraints Parameter</i>	43
4.4	<i>Material Properties Parameter</i>	44
4.5	<i>Temperature Parameter</i>	46
4.6	<i>Thickness Parameter</i>	48
	Conclusions and Perspectives	50
	<i>Numerical Improvement of the Model</i>	50
	<i>Non-numerical Developments</i>	51
	References	53
	Appendix	55
	<i>Thermal Environment Script</i>	55
	<i>Interpolation Program</i>	55
	<i>Solving Script</i>	57
	Summary in italian	59

Acknowledgements

I would like to thank my supervisor Prof. Fabrizio Dughiero for giving me the opportunity to work on this thesis abroad.

I would also like to thank the whole team of the *Institut für Elektroprozessstechnik* (ETP) for hosting me at *Leibniz Universität Hannover* during the last semester. A particular thank goes to my foreign supervisor Prof. Egbert Baake, to Dr. Alexander Nikanorov who helped me with the FEM simulations and to my other colleagues M.Sc. Martin Schulze, M.Sc. Marco Baldan and M.Sc. Mattia Guglielmi.

My gratitude goes to my family, in particular to my parents Mauro and Cinzia and to my sisters Anna and Camilla, who always supported me through my university years.

I would also like to praise all the friends, old and new, who took part into this parenthesis of my life.

Introduction

Nowadays, the main industrial methods for the continuous heating and treatment of metal strips are gas-fired and electrical resistance furnaces. In this context, induction heating represents a valid alternative. Indeed, the traditional ways are time-consuming in terms of heating and preheating times, not energetically efficient and not flexible.

Induction heating, both longitudinal flux heating (LFH) as well as transverse flux heating (TFH), makes possible to tackle all these issues; it allows to reach very high power densities, reducing the heating time, and it has an higher energy efficiency (up to 95%).

Talking about flexibility, TFH gives the possibility to work with different strip dimensions and thicknesses by means of simple inductor geometry modifications. It is possible due to the process configuration; in TFH the inductor is open, as it is placed above and under the workpiece, and it is possible to freely operate on it in order to adapt it to any strip to heat or to treat.

Conversely, it is important to underline also TFH issues. The main one is the difficulty to control the temperature homogeneity during the process. This leads to two important drawbacks: it can cause non-uniformity in the treatment of a metal piece, but it can also produce deformations, vibrations and thermal buckling during the process itself.

The focus of this work will be set particularly upon the simulation of the buckling behaviour of a metal strip heated by means of TFH. The decision to investigate in this direction arose from both experimental and industrial evidences of instability during this kind of heating processes.

Since the difficulty of a physical collection of data appears to be clear from the beginning, the chosen way to investigate was a finite element simulation of the phenomenon. The purpose during the creation of the numerical model was, more than to simulate the experimental evidences (which are too unstable), to create a buckling analysis tool which produces reasonable and consistent results. In particular, the effect of the variation of different parameters like boundary conditions, material properties and other model inputs will be considered.

The FEM model developed could be useful to predict the effect of different parameters upon the buckling phenomenon. Another possible outcome of this simulation could also be to become part of a wider multi-physical simulation (i.e. by combining it with an electromagnetic simulation).

In this way it would be possible to get a bigger frame of a transverse flux heating leading to a further optimization of the process.

The investigation started with an ideal model which embodied the homogeneous heating of the strip. Later on, the temperature field resulting from an electro-magnetic analysis was implemented. The results obtained by these two simulations are comparable and stable.

Structure of the thesis

This thesis will be divided in 4 chapters:

- **Chapter 1: Preliminary notions.** In this chapter the whole necessary knowledge about transverse flux heating and thermal buckling will be provided.
- **Chapter 2: The FEM simulation.** This chapter will be dedicated to the explanation of Multiphysics simulation and to the particular simulation tools used in this work.
- **Chapter 3: The numerical model.** In this chapter the construction and development of the studied numerical model will be shown and explained.
- **Chapter 4: Parametrical Analysis.** The effect of the variation of several physical parameters will be studied in this chapter. The results of this parametrical analysis will be shown as well.
- **Conclusions and perspectives.**

1 Preliminary notions

1.1 Induction heating principles

Induction heating processes in industrial application, particularly in the frame of metal strips heating and treatment, are a more than valid alternative to conventional furnaces (i.e. gas-fired, electrical resistance, etc). The main advantages of induction heating could be summarised as it follows:

- The heat is produced directly inside the workpiece, so that no heat transfer through a medium is required.
- The possibility to reach high power densities. It implies quicker heating times.
- High efficiency, in particular, dealing with high resistivity or ferromagnetic metals
- The flexibility of the process. In terms of optimisation of the inductor geometry in order to improve the coupling with the workpiece.
- Induction heating processes allow high repeatability.
- It reduces the amount of CO₂ emissions compared to other processes.
- The overall energetical efficiency is higher than traditional processes.

The induction heating process and its main components will be briefly described. The main component of the process is the coil or inductor and it is usually made of conductive materials. An electrical current flows inside the inductor generating a magnetic field. One of the current main parameters is the frequency, it is important to point out the huge role of this parameters in induction heating. The entity of frequencies used could really characterise the process; the use of very high frequencies is necessary in processes like surface treatments, while low frequencies are usually more used for through heating processes.

The variation of current creates a variation of the magnetic field. The time variation of the magnetic flux generates an electromotive force that works as a voltage applied to the workpiece. This voltage generates currents inside the workpiece, which are called induced currents or eddy currents. These currents are responsible of the heating according to Joule's effect.

The uniformity of the heating depends directly upon the distribution of the induced currents. It is really hard to get a completely uniform currents distribution; the reasons behind that are the non-uniformity of the magnetic field inside the inductor and the, so-called, skin effect.

According to the skin effect, the currents tend to distribute themselves inside the workpiece; in particular, the current density is higher on the external surface and presents an exponential decay toward the centre. It will be essential to keep that in mind while working with longitudinal flux induction heating.

It is useful to define a certain penetration depth (δ) of the eddy currents; it is a function both of the process (in terms of frequency) and of the material properties (in terms of resistivity and permeability).

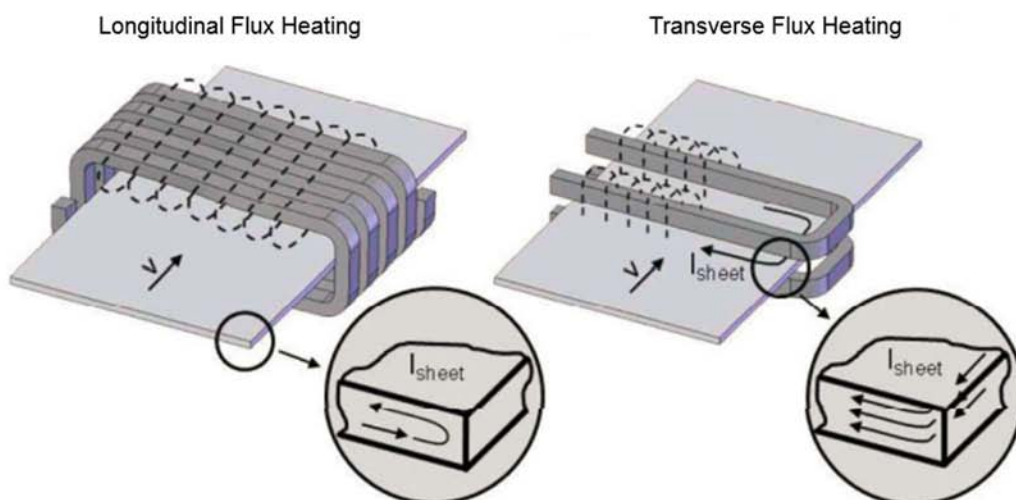
$$\delta = \sqrt{\frac{\rho}{\pi\mu f}} \quad (1)$$

Where:

- δ is the penetration depth;
- ρ is the electrical resistivity;
- μ is the magnetic permeability;
- f is the frequency.

1.2 Induction heating processes

The two main techniques of induction heating are Longitudinal Flux Induction Heating (LFH) and Transverse Flux Induction Heating (TFH). Even if they both share the pros and cons explained in the previous chapter (§1.1), they also present some critical differences.



Before comparing these two technologies, a quick overview of them will be presented.

In the more common Longitudinal Flux Heating (LFH), the workpiece is placed inside the inductor (usually a solenoid) and so immersed in a magnetic field that is parallel to the axis of the solenoid (see ‘Longitudinal Flux Heating’ in *Figure 1.1*). This configuration is characterized by the skin effect; the eddy currents flow in the cross-section of the workpiece with a certain penetration depth (1). LFH configuration allows, by means of a frequency variation, to carry out both surface- and through-heating.

The limit of LFH could be the small value of the thickness of the workpiece. Due to the fact that the penetration depth decreases with higher frequencies, it becomes necessary to use really high frequency for the correct heating of a thin strip. The ratio between the penetration depth and the diameter/thickness of the workpiece must always be around 3,5. If this ratio is smaller, it is possible that the induced eddy currents cancel each other and so the proper heating of the strip is not feasible. This problem could be solved only by using extremely high frequency generators which are usually expensive. So, the main drawback in using this technology for metal strip heating would be the costs. However, by using the right frequency, LFH is still an efficient process.

In the typical set-up for Transverse Flux Heating (TFH), instead, the workpiece passes through an open inductor which is, in the case of a metal strip, placed above and below it (‘Transverse Flux Heating’ in *Figure 1*). This inductor configuration allows to have a magnetic field perpendicular to the workpiece. In this way the induced currents flow on the surface of the workpiece and so the whole cross-section is invested by them; this is the reason why only through-heating of the workpieces can be reached. Due to this peculiarity, the process can be used for the treatment of workpieces with a large spectrum of thicknesses.

In the case of TFH there is not any skin effect on the heated piece. So, not being necessary to get really high with frequencies to reduce the penetration depth, lower frequencies and so less

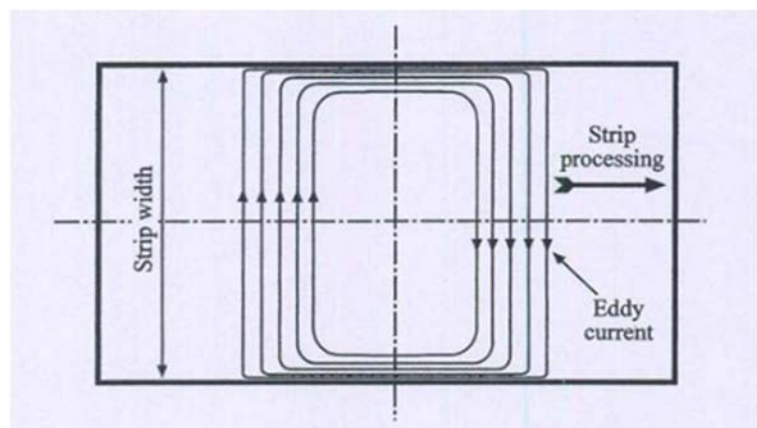


Figure 1.2 – Eddy currents path in TFH

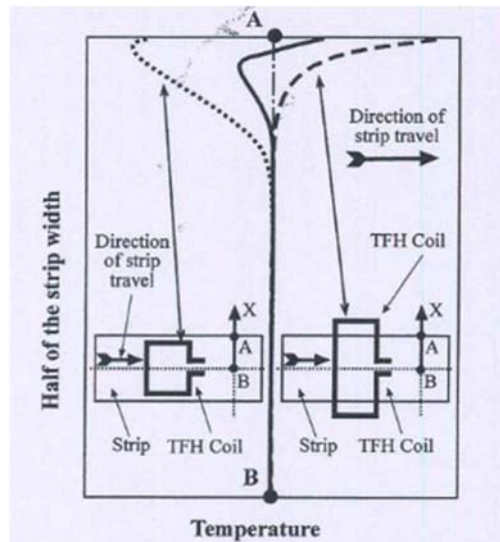


Figure 1.3 – Typical temperature profiles in TFH, according to the inductor width variation

expensive processes can be carried out.

In contrast, TFH has also a few not negligible drawbacks; it is hard to achieve an uniform temperature distribution and some mechanical phenomena, as vibrations, deformations, noise, buckling, can occur during the heating process.

The main issue about the temperature homogeneity is the so-called *edge effect*. In TFH the shape of the inductor deeply affects the currents paths in the strip; in particular, the currents tend to reflect the shape of the inductor. If the coil is wider than the heated strip, the induced currents are not able to follow the inductor path and so they are “pushed” on the edge of the strip (*Figure 1.2*). This concentration of currents could provoke an overheating of the edges of the strip. The contrary is true as well; if the inductor is too small, compared to the strip width, there will be a lack of current density on the edges and so they will be underheated (*Figure 1.3*). This inhomogeneity in the transversal direction, in respect to the direction of motion of the strip, could be the possible main cause of the mechanical phenomena mentioned above.

The most direct way to deal with temperature distribution is by optimizing the design of the inductor. This optimization can be developed in two ways: by modifying of the inductor shape and/or by parametrically studying the process variables.

In both cases the main variables of the system to be considered are:

- The conductor distance or pole pitch;
- The dimensions of the conductor itself;
- The air gap;

The shape optimization can be carried out via FEM simulations having the temperature homogeneity as goal. This kind of electro-magnetic simulation must take into account the heated material properties as well. In particular, it is important to implement non-linear properties in order

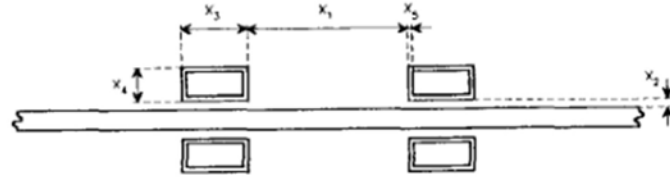


Figure 1.4 – Transverse-flux Induction heating system scheme

to get more accurate results. The most outstanding obtained result was the reduction of the deviation from the target temperature from 15% to 3%, by means of an inductor shape modification.

As far as it concerns the parametrical study of the process variables, the inductor can be further parametrized, as in *Figure 1.4*. Where:

- x_1 = conductors distance;
- x_2 = airgap length;
- x_3 = conductor length;
- x_4 = conductor height;
- x_5 = conductor thickness;
- x_6 = system frequency

By parametrical study it means to identify an “objective function” of a vector that includes all these independent variables. In this case the goal of the process is to improve the efficiency of the coupling inductor-workpiece by means of modifications of the coil parameters.

In both cases, it appears clear how the optimization of the shape design of the inductor has a remarkable effect upon the process efficiency and on the heating uniformity.

1.3 Strip deformation in TFH

In this section the effect of temperature gradients upon the strip deformation will be discussed. It is well known that the existence of a non-uniform temperature field in a metal piece or strip leads to thermal stresses. The entity of these stresses depends not only on the entity of the temperature

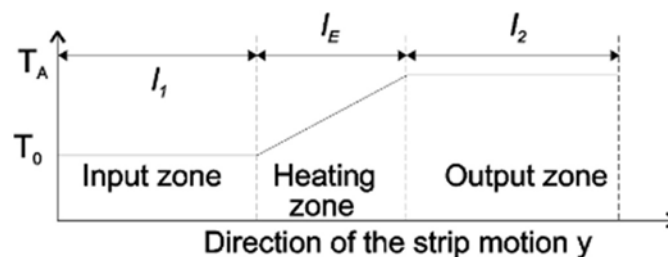


Figure 1.5 – Strip different temperatures

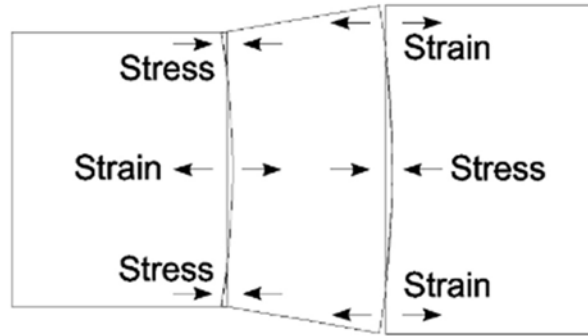


Figure 1.6 – Directions of the stresses and strains

gradient, but also on materials' properties such as Young modulus and coefficient of thermal expansion. See formula (2), where:

- σ = thermal stress;
- E = Young's modulus;
- α = coefficient of thermal expansion;
- ΔT = temperature gradient.

$$\sigma = E\alpha(\Delta T) \quad (2)$$

In the frame of transverse-flux induction heating, the presence of thermal stresses becomes an issue once it provokes the deformation or the buckling of the strip.

It is possible to schematize the TFH process as the simple heating of a strip from an initial temperature T_0 , in the input zone, to a final temperature T_A , in the output zone (*Figure 1.5*). Among these two zones, input and output, as the temperature of the strip is constant, there will be no deformations. If the strip is free to deform, it will do it in the central/heating zone. This deformation will lead to stresses on the boundaries, as it is shown in *Figure 1.6*.

Theoretically, this portion of the strip, the heating zone, will be more easily predisposed to buckling. This fact will be an important parameter for the qualitative evaluation of the buckling simulation that will be discussed later.

Another important theoretical consideration regards the strip thickness; thinner strips would incur in buckling more easily than thicker ones. Furthermore, the buckling would not take place in strips thicker than a certain critical value. The entity of this threshold depends upon the characteristics of every single system.

Another possible cause of the deformation/buckling of a thin strip could be vibrations. The origin of vibrations can be mechanical, as the result of the strip movement system itself, but it can also be magnetic. In transverse flux heating, in particular, the portion of material subjected to magnetic

forces is bigger than in LFH, so vibrations could be an issue. While on the subject, it should be acknowledged that, as vibrations are strictly related to the frequency, only by working at very low frequencies the phenomenon would be visible.

1.4 Applications of TFH - Example

The most common industrial application of TFH can be found in the metal industry. In particular, it is used for the annealing or for the heating of metal strips, usually as a part of a bigger in-line process.

An interesting recent application of it can be found among DUE™ process (Danieli Universal Endless). In this case, the induction heating station is devoted to the homogenization of the temperature of a metal strip between two subsequent milling stations. One of the main advantages of this technology, in comparison with the traditional ones (gas-fired and resistance furnaces), is the reduction of the physical occupied space. Furthermore, it is also a good example of versatility of the process as the company must deal with various strip thicknesses.

1.5 Buckling Phenomenon

Even though the phenomenon of buckling is yet to be well understood, it is nowadays a failure cause not to be neglected. The opposite is true: buckling must be taken into account in the designing

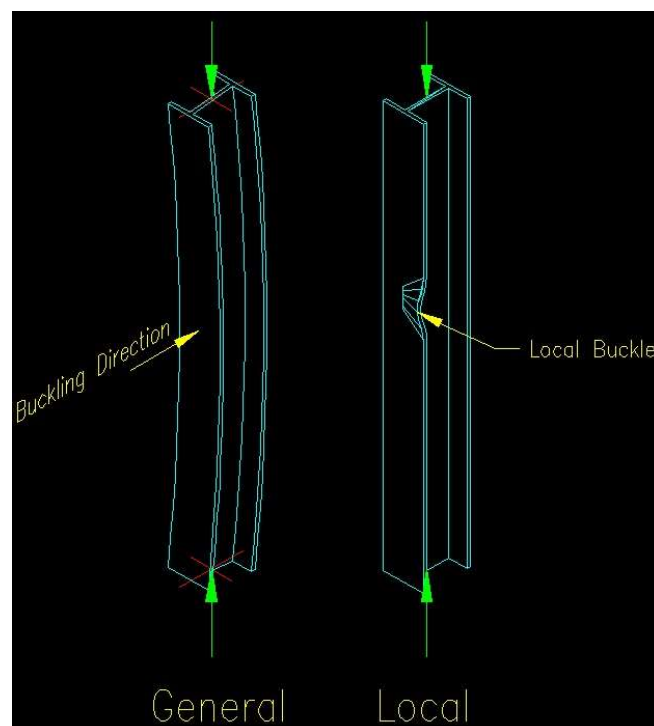


Figure 1.7 – General vs Local Buckling

of structural pieces, processes, as well as of machineries and other final products.

It is possible to classify two main buckling modes: general buckling and local buckling. The former is a distortion of the axis of the studied piece. Local buckling is, instead, the distortion of a component of the cross section without any axis distortion (*Figure 1.7*).

It is possible to predict the incurrence of buckling in terms of the individuation of a critical stress value. The most direct method is the application of Euler's equation; in equation (3) a generic formulation is given.

$$\sigma_{cr} = E \left(\frac{\pi}{S} \right)^2 \quad (3)$$

Where:

- σ_{cr} is the critical Euler's stress
- E is the Young's modulus
- S is the slenderness of the component

It appears clear from equation (3) that a high value of slenderness should be avoided. In the case of metal strips, it can be translated into avoiding, as much as possible, very small thicknesses. Usually, the critical stress value for buckling is lower than the yield limit of a certain material; that is the reason why it could be dangerous not to consider buckling failure.

As it concerns thermal buckling, the cause of the phenomenon can be identified, with a certain degree of certainty, with the temperature gradients created in the workpiece.

The temperature difference is not enough by itself; the other necessary factor would be the state of stress. The thermal expansion must be somehow restrained in order to get thermal buckling, if it is not, and the component is free to deform, the thermal stresses would not induce buckling but only the thermal expansion would occur.

As an example, studying a heated steel strip in a continuous annealing furnace, the buckling happens as a combination of temperature distribution, line tension and friction between the strip and the rollers. The shape of the rollers, in an annealing furnace, might have an effect upon buckling as well; it has been studied how different roller shapes influence the deformation behavior of the metal strip, as they probably alter the state of stress of the metal strip.

2 The FEM Simulation

The purpose of this chapter is to present a brief overview of Multiphysics simulations. Secondly, the tools, provided by the software ANSYS Mechanical APDL® (release 19.2), for performing a buckling analysis will be introduced.

2.1 Multiphysics simulations

The word Multiphysics commonly refers to the process of simulation of multiple coupled and interacting physical phenomena. This procedure is becoming increasingly spread in the field of computer aided engineering, virtual prototyping and product design. Even though the possibility to carry out Multiphysics simulation requires an increased computer capability, it might be more time and computationally efficient than coupling single simulations. The coupling of single simulations might bring to some new limitations in terms of stability, accuracy or robustness, more than it happens in the single simulations. This fact is mainly due to the conversion of data needed between different and independent simulations.

Typically, a Multiphysics system is formed by different components characterised by its own principles (conservation and/or constitutive laws). A few examples could be the coupling of:

- Radiation with hydrodynamics (RHD)
- Electricity and magnetism with hydrodynamics (Magnetohydrodynamics - MHD)
- Chemical reaction with transport (reactive transport)

Many other combinations are feasible to simulate the interactions among structural mechanics, heat transfer, fluid flow, electromagnetics, etc...

Historically, Multiphysics has been considered as a series of single-physics simulations; each one focused on a separate field of study (fluids, structural, thermal, electronics). Nowadays it is necessary to take into account the effect of different physical forces simultaneously; only this way allows to investigate and simulate real-world product failures and behaviours. The first step into Multiphysics has been to connect multiple simulations; this process has become during the years

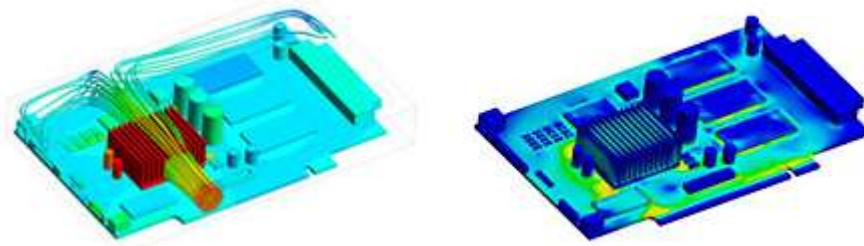


Figure 2.1 – Example of coupled heat transfer and thermal stress analysis

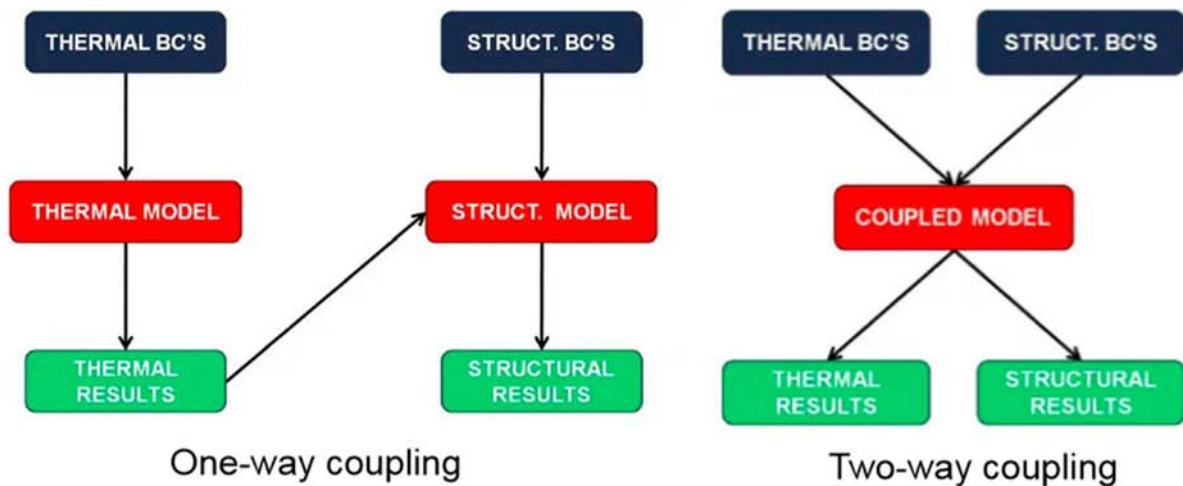


Figure 2.2 – Schematization of one-way and two-way coupling in Multiphysics simulations.

more efficient and accurate. The turning point has been the capability to transfer initial and boundary data between the different steps without losing fidelity and accuracy and, furthermore, without introducing new errors. It is possible to refer to this way of operating by *sequential* or *one-way coupling*. In sequential coupling the so-called partitioned approach is applied; it means that the equation regarding the single physics are solved separately and then coupled suitably.

Sometimes the physics, that have to be coupled, present strong interactions that cannot be simulated sequentially. In this case, it becomes necessary to run concurrent simulations, implementing also the possibility to exchange data between them at specified time intervals. This more sophisticated analysis is called *two-way co-simulation* or *direct coupling*. Direct coupling is often a single matrix system wherein the equations concerning all the physics involved in the simulation are solved together.

In order to better understand the distinction between these two types of Multiphysics, one example of thermal-structural coupling is provided in *Figure 2.2*.

2.2 Buckling analysis in ANSYS Mechanical APDL®

In order to perform the thermal and structural analysis, ANSYS Mechanical APDL® (release 19.2) was used. The software provides two main tools to perform buckling analyses: linear eigenvalue buckling analysis and non-linear buckling analysis.

The first one is the quickest and easiest method; it provides the deformed shape and calculates the buckling factor. This factor is useful to estimate the critical buckling load as this value is given by

the applied load multiplied for the buckling factor itself. The eigenvalue (or bifurcation point) calculated by the program matches the theoretical solution of Euler's buckling equation. Concerning the critical stress value, results from the eigenvalue linear analysis are to be considered non-conservative; this tool does not take into account the presence of imperfections and nonlinearities typical of real-world structures. Even if the displacements obtained do not have physical meaning, they offer anyway a qualitative representation of the different buckling modes. The number of buckling modes taken into account in the analysis deeply affects the results. There is not any evidence about the meaning ANSYS® gives to the number of buckling modes. But it is plausible that it refers to the theoretical number of half waves, even if it is not to specify the direction of them.

It is possible to get more realistic results using the non-linear buckling analysis. This tool consists of a static structural analysis where the load is applied incrementally and large displacements are allowed (command NLGEOM,ON). In order to obtain buckling using this method, some "imperfections" should be included in the model to trigger it. Possible imperfections could be geometrical defects or an out-of-plane load application. The implementation of such imperfections is a delicate step as it is not easy to determine either where to add an out-of-plane load or what defect to introduce in the geometry. A good compromise is to use the deformed shape obtained with an eigenvalue linear analysis as starting geometry. It is possible to do so in ANSYS® (command UPGEOM); the software also offers the possibility to set a maximum displacement to be used for this operation. This is an important assumption in the model and the effect of that will be discussed later.

In the studied case, thermal buckling was considered. A preliminary thermal analysis is carried out in order to determine the state of stress. The result from the thermal analysis is then used as the loading step for the buckling one.

As a first stage of the work, an homogeneous heating zone has been considered. The next step was to use the thermal field resulting from a previous Electromagnetic/Thermal analysis instead. This combined analysis was previously carried out on the same inductor/workpiece system in order to define the best shape of the inductor to be used.

2.2.1 The choice of the Element Type in the FEM analysis

The preliminary eigenvalue linear analysis was carried out both with SOLID and SHELL elements. The two types of mesh produced similar results. But, as the analysis moved on to the non-linear

buckling, SHELL elements happened to be more stable and gave more realistic results.

In order to perform a combined analysis (Thermal and Structural) two compatible elements, in terms of number of nodes per element (4 nodes), were used: SHELL157 (thermal) and SHELL181(structural). The first one presents two degrees of freedom: voltage and temperature. SHELL181 presents, instead, 6 degrees of freedom: displacement in x, y and z direction and rotation around axes x, y and z. SHELL157 may result useful once a preliminary electromagnetic analysis should be performed.

For the thermal analysis it was considered also the element SHELL131, which is a pure thermal element. Since no significant differences were found (same deformed shape and stress distribution and maximum stress intensity difference equal to 3%) SHELL157 was chosen thanks to its higher versatility for combined analysis. Conversely, it could be useful to switch to the element SHELL131 whenever a layered analysis is needed.

For the analysis with solid element, SOLID70 (thermal) and SOLID5 (structural/buckling) were used.

2.2.2 Solving Equations

The shape functions associated to the elements used are listed below.

$$u = \frac{1}{4}(u_I(1-s)(1-t) + u_J(1+s)(1-t) + u_K(1+s)(1+t) + u_L(1-s)(1+t)) \quad (2)$$

$$v = \frac{1}{4}(v_I(1-s) \dots (\text{analogous to } u)) \quad (3)$$

$$w = \frac{1}{4}(w_I(1-s) \dots (\text{analogous to } u)) \quad (4)$$

$$\theta_x = \frac{1}{4}(\theta_x(1-s) \dots (\text{analogous to } u)) \quad (5)$$

$$\theta_y = \frac{1}{4}(\theta_y(1-s) \dots (\text{analogous to } u)) \quad (6)$$

$$\theta_z = \frac{1}{4}(\theta_z(1-s) \dots (\text{analogous to } u)) \quad (7)$$

$$T = \frac{1}{4}(T_I(1-s) \dots (\text{analogous to } u)) \quad (8)$$

$$V = \frac{1}{4}(V_I(1-s) \dots (\text{analogous to } u)) \quad (9)$$

$$\phi = \frac{1}{4}(\phi_I(1-s) \dots (\text{analogous to } u)) \quad (10)$$

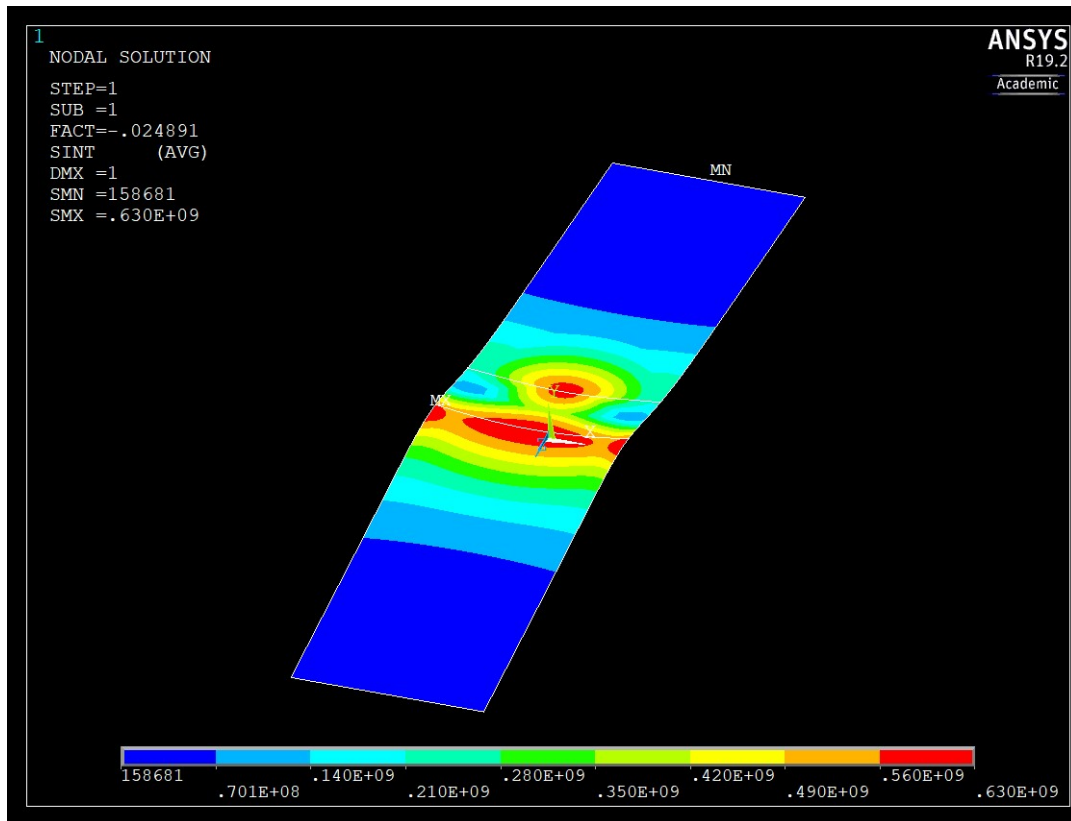


Figure 2.3 – Linear eigenvalue analysis with Block Lanczos extracting method; number of buckling mode: 1.

The linear eigenvalue buckling analysis is based upon the calculation of the eigenvalue in the following equation (11).

$$[K][\phi_i] = \lambda_i[M][\phi_i] \quad (11)$$

Where K is the structural stiffness matrix, that includes the stress stiffness matrix for prestressed analysis, ϕ is the eigenvector, λ is the eigenvalue and M is the structural mass matrix.

The eigenvalues can be calculated in ANSYS with two methods:

- The Block Lanczos Extraction method, which is preferable for large models and symmetric problems
- The Subspace Iteration Method, which uses the same solving algorithm as the Ansys Unsymmetric Method. These methods are indicated for solving models with unsymmetrical matrices.

As far as it concerns the studied thermal buckling problem, the two methods provide almost identical results. These results are shown in *Figure 2.3* (Block Lanczos Extraction Method) and *Figure 2.4* (Subspace Iteration Method). The two pictures show the stress intensity resulting from a linear eigenvalue buckling analysis. In this case the number of buckling modes used was equal to 1.

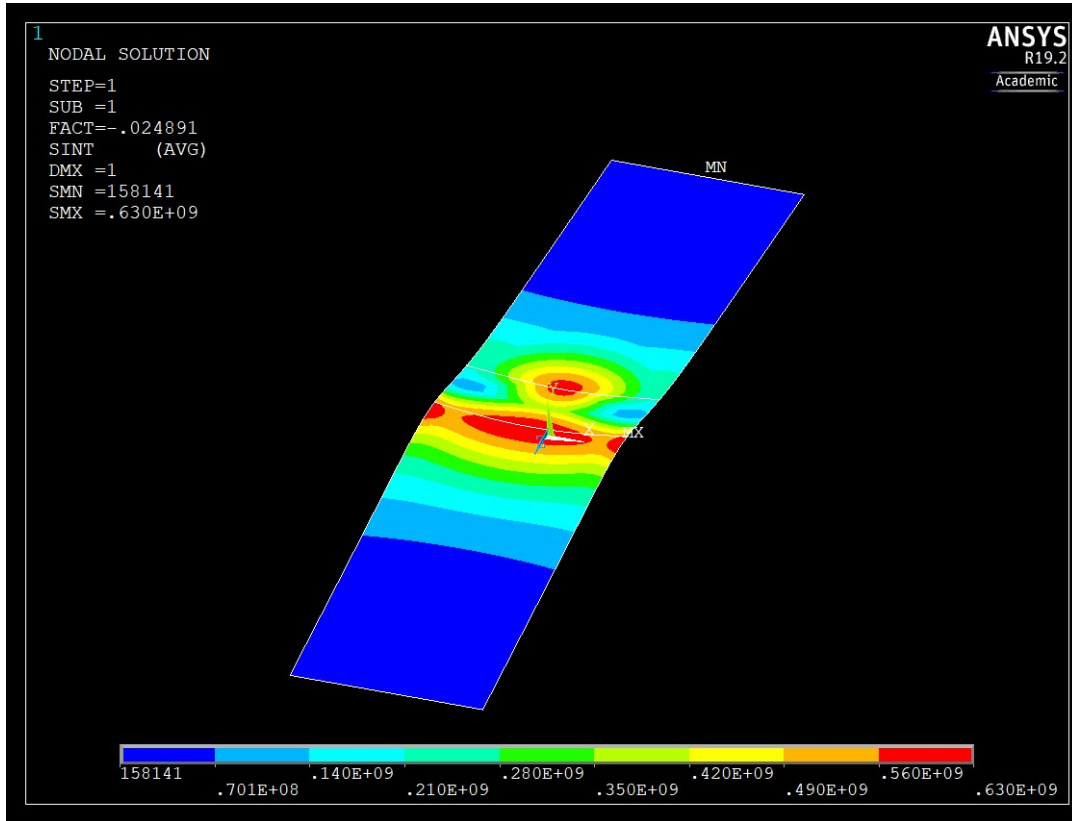


Figure 2.4 - Linear eigenvalue analysis with Substep Iteration extracting method; number of buckling mode: 1.

3 The numerical model

3.1 General Description

The process to be simulated is the transverse-flux induction heating of a metal strip. The numerical model simulates a continuous process: the metal strip moves through the inductor, as it would happen if the inductor is a step of a bigger in-line process (i.e. preheating before mechanical deformation).

In order to simulate the described process an increasing temperature profile is applied to a rectangular strip with a certain thickness. In this way it was possible to simulate the temperature transient during time via a spatial distribution. As a first approximation an homogeneous heating has been considered; the heating zone is the portion of strip theoretically covered by the inductor. In the meantime, one end of the strip is maintained at room temperature and the other one at a fixed temperature, which can be varied.

Afterwards, the temperature distribution resulting from an electro-thermal analysis was used. In order to do this, it was necessary to develop a code to interpolate the temperature field to make it fit with the model mesh.

In order to carry out the analysis, the strip must be somehow fixed; multiple constraints' configurations have been explored. Finding the best constraints' configuration it is, indeed, one of the most delicate part of the simulation as it is hard to transpose the reality of the constrains into the numerical model.

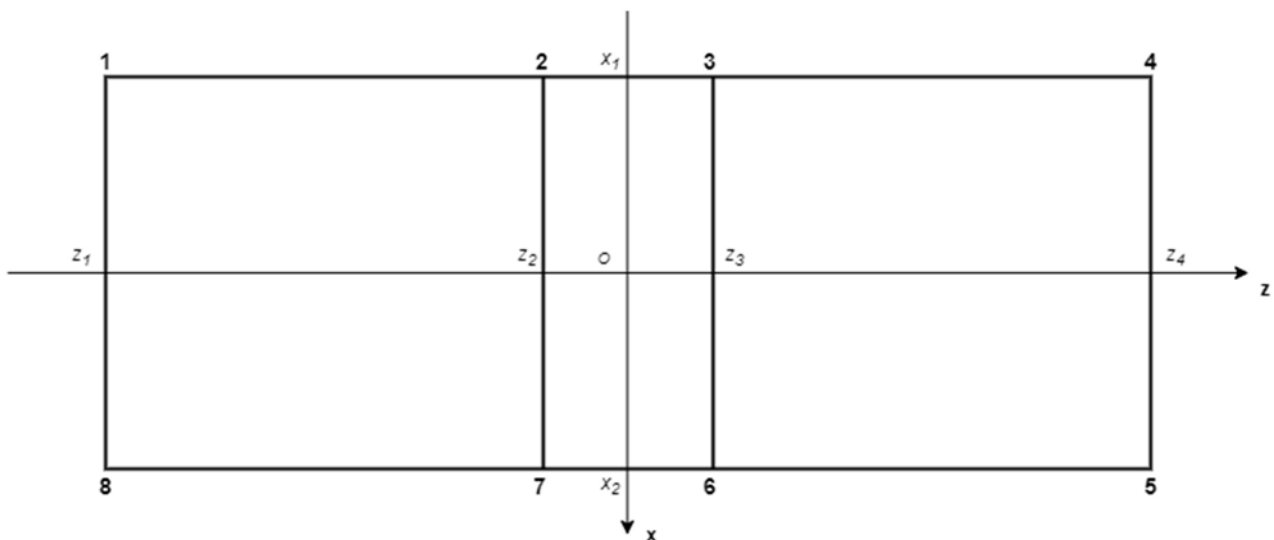


Figure 3.1 – KeyPoints scheme.

3.2 Model Construction

This paragraph will follow the construction steps of the model; each step will be presented alongside with the code implemented.

3.2.1 Model Geometry

The main purpose in the construction of the geometry of the strip was to implement the possibility of quick and simple modification of it. This goal has been achieved via the construction of a parametric geometry. As the model is not complex, it is possible to write this parametric code directly inside ANSYS® environment.

The geometry is based upon cartesian coordinates (x,y,z) . In the studied case, the direction of motion of the strip, along the z axis, were chosen in order to be consistent to the results of previous electromagnetic-thermal coupled simulations that will be used later in the model.

By the way, the choice of the axes can be arbitrary and, if needed, it is possible to rotate the geometry by simply changing the coordinates.

The geometry was built by using KeyPoints (KPs) which are defined by a set of cartesian coordinates (x_n, y_n, z_n) . The position of these points relied upon the scheme shown in *Figure 3.1*. The values of the coordinates are simply determined as input data.

```

/prep7
/plopts,date,0
emunit,mks
eps=1.0E-08
! Input Data
x1=-400/1000
x2=400/1000
y0=0
z1=-2000/1000
z2=-200/1000
z3=200/1000
z4=2000/1000
thk0=1.4/1000
csys,0
! Definition of the KeyPoints
k,1,x1,y0,z1
k,2,x1,y0,z2
k,3,x1,y0,z3
k,4,x1,y0,z4
k,5,x2,y0,z4
k,6,x2,y0,z3
k,7,x2,y0,z2
k,8,x2,y0,z1
kselect,all
kplot

```

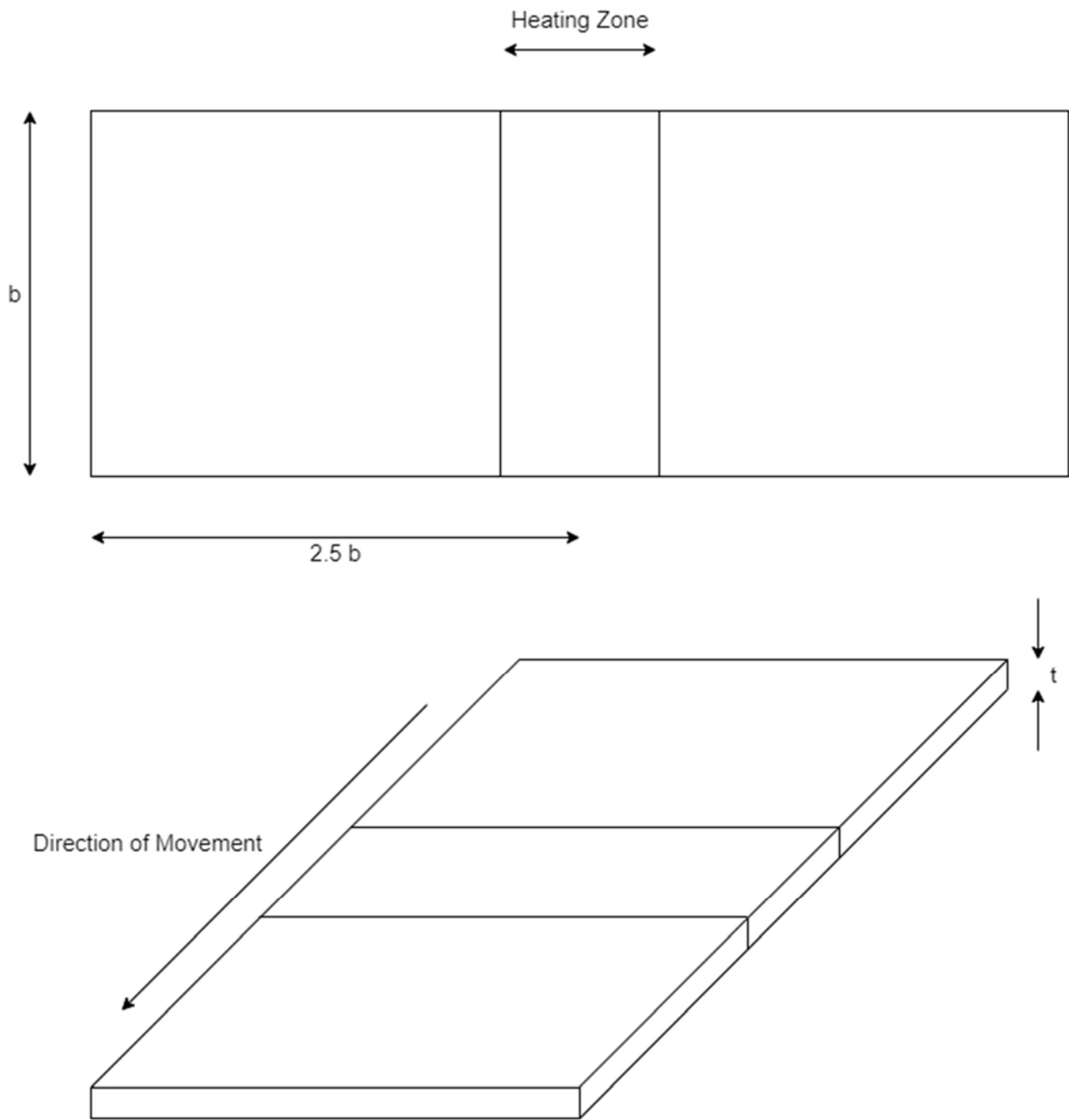


Figure 3.2 – Scheme of the model

The benchmark dimensions ('Input Data' in the code) are:

- Width = $b = 800\text{mm}$
- Length = $2,5 \cdot b = 2000\text{mm}$
- Heating zone length = 400 mm
- Thickness = $1,4\text{ mm}$ (' t_{hk0} ' in the code)

The benchmark geometry scheme is shown in *Figure 3.2*.

Having defined the coordinates of the points, to build the solid 3D strip, lines and areas were attached to the KPs. The third dimension, the one defining the thickness of the strip does not need to be given as the other two dimensions (via KPs, lines and areas definition); it is implemented as a property of the shell elements that were used. So that the only input data needed is the value of the thickness itself (thk0).

```
! Definition of lines in the 'x' direction
```

```
lstr,1,8
lesize,all,,,nx1,nx1n
lstr,2,7
lesize,all,,,nx1,nx1n
lstr,3,6
lesize,all,,,nx1,nx1n
lstr,4,5
lesize,all,,,nx1,nx1n
```

```
! Definition of lines in the 'z' direction
```

```
lstr,1,2
lesize,all,,,nz1,nz1n
lstr,8,7
lesize,all,,,nz1,nz1n
```

```
lstr,2,3
lesize,all,,,nz2,nz2n
lstr,7,6
lesize,all,,,nz2,nz2n
```

```
lstr,3,4
lesize,all,,,nz3,nz3n
lstr,6,5
lesize,all,,,nz3,nz3n
```

```
lsel,all
lplot
```

```
! Definition of the areas
```

```
a,1,2,7,8
a,2,3,6,7
a,3,4,5,6
```

```
asel,all
aplot
```

```
asel,all
aglu,all
```

```
asel,all
aplot
```

```
finish
```

This fragment of code shows how lines and areas were created; the process is the simple connection between the already-defined KPs. The values nx1, nz1, nz2, nz3 are needed to define the number of

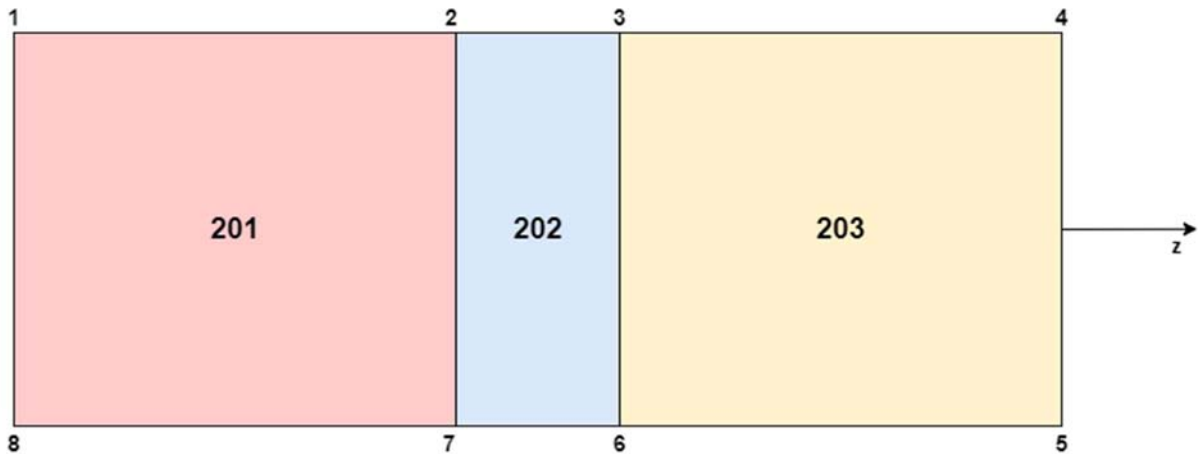


Figure 3.3 – Areas with assigned attributes number.

mesh elements per line. The meshing of the model will be discussed in §3.4.

The model is a coupled thermal and structural analysis, but the same geometry can be used in both the single physics by simply resuming it between the different simulation steps.

3.2.2 Attributes of the elements

Once the geometry was created, attributes must be given to the elements constituting it. As attributes they are included: the mesh, the element type and the material properties. The procedure simply consists in assigning an identification number to the investigated areas and then associating

```

/prep7
csys,0

! Selection of areas and attributes number assignment
ksel,s,,,1,2
ksel,a,,,7,8
lslk,s,1
asll,s,1
aatt,201,1,201

ksel,s,,,2,3
ksel,a,,,6,7
lslk,s,1
asll,s,1
aatt,202,1,202

ksel,s,,,3,6
lslk,s,1
asll,s,1
aatt,203,1,203

asel,all
aplot
finish

```

meshing and properties to that number.

By doing this it would be also possible to implement, in the code, pieces/geometries that include parts made of different materials. That is the reason why the studied areas are differently designated between each other's (*Figure 3.3*).

In the next step the element type is assigned to each area; as it happened before, it is possible to assign different element types to different areas if needed. As far as it concerns the choice of elements for the studied model refer to §2.2.1.

```

/prep7
SHPP,OFF
! Element type assignment
  et,201,shell181
  et,202,shell181
  et,203,shell181
  r,1,thk0,thk0,thk0,thk0,,
! Elements options definition
keyopt,201,8,2
keyopt,202,8,2
keyopt,203,8,2
keyopt,201,3,2
keyopt,202,3,2
keyopt,203,3,2
! Mapped mesh implementation
asel,s,mat,,201,203
mshape,0,2d
mshkey,1
amesh,all
esel,all
eplot

finish

```

The fragment of code displayed here concerns the structural analysis elements; the element type chosen is the SHELL181, SHELL157 was used for the thermal analysis instead. The 'keyopt' command is used to defined elements properties in order to improve the model accuracy. As it was said talking about the model geometry (§3.2.1), thickness is simply an element parameter which is implemented in this phase.

Concerning the meshing operations, for the studied model a mapped mesh was chosen. All the data about it are provided during the geometry construction phase (lines definition) as well as input data:

```

nx1=57
nx1n=1
nz1=60
nz1n=0.25
nz2=29
nz2n=1
nz3=60
nz3n=4.25

```

The remaining attribute to be assigned is the material properties. The procedure is straightforward; the properties are simply defined and linked to the areas designation number. Similarly to what happened with meshing and element type, the material properties can be differentiated between different sections. The definition of material properties will be further discussed in §4 – *Parametrical Analysis*.

The fragments of code regarding the properties are displayed below. In the order, the two parts refer to the properties needed for the thermal analysis and the ones for the structural analysis. Properties like thermal conductivity, specific heat and density are in common and displayed only in the first fragment.

```

! Workpiece material: steel C455
/prep7

! Definition of thermal conductivity
mptemp
mptemp,1, 0, 20, 100, 200, 300, 400, 500, 20000
mpdata,kxx,2,1, 16, 16, 18, 19.7, 21.3, 23.4, 24.7, 24.7

! Definition of specific heat
mp,c,2,500

! Definition of density density
mp,dens,2,7760

    mpcopy,,2,201
    mpcopy,,2,202
    mpcopy,,2,203
finish

```

```

! Workpiece material: steel C455
/prep7

! Definition of Young's modulus
mptemp
mptemp,1, 0, 20, 200, 20000
mpdata,ex,2,1, 2e+11, 2e+11, 1.88e+11, 1.88e+11

! Definition of the Coefficient of Thermal Expansion
mptemp
mptemp,1, 0, 93, 100, 200, 300, 480, 200000
mpdata,alpx,2,1, 10.6e-6, 10.6e-6, 10.9e-6, 11.5e-6, 11.7e-6, 12.0e-6,
12.0e-6

! Definition of Poisson's ratio
mp,prxy,2,0.30
tnostress=20.0
mp,reft,2,tnostress
    mpcopy,,2,201
    mpcopy,,2,202
    mpcopy,,2,203
finish

```

3.3 Model boundary conditions

After the construction of the geometry and the definition of the elements attributes, it is necessary to define the boundary conditions of the model. In order to achieve this, two different environments were created; one regarding the thermal simulation and another regarding the structural one.

3.3.1 Thermal environment

Thermal environment means the temperature profile that has to be applied at the workpiece. Initially, the profile used was an homogeneous heating taking place in the central zone of the strip; In this way it was simulated the heating effect of an ideal inductor. In particular, the temperature is constant until the heating zone and it is equal to room temperature. The last sector of the strip is considered at a steady temperature. The value of this last temperature can be modified according to the treatment to be carried out or the material analyzed.

In the code the thermal environment is formed of three main parts:

1. Recalling of input data, geometry, meshing and material properties;
2. Definition of the ANSYS® analysis type;
3. Definition of the temperature profile.

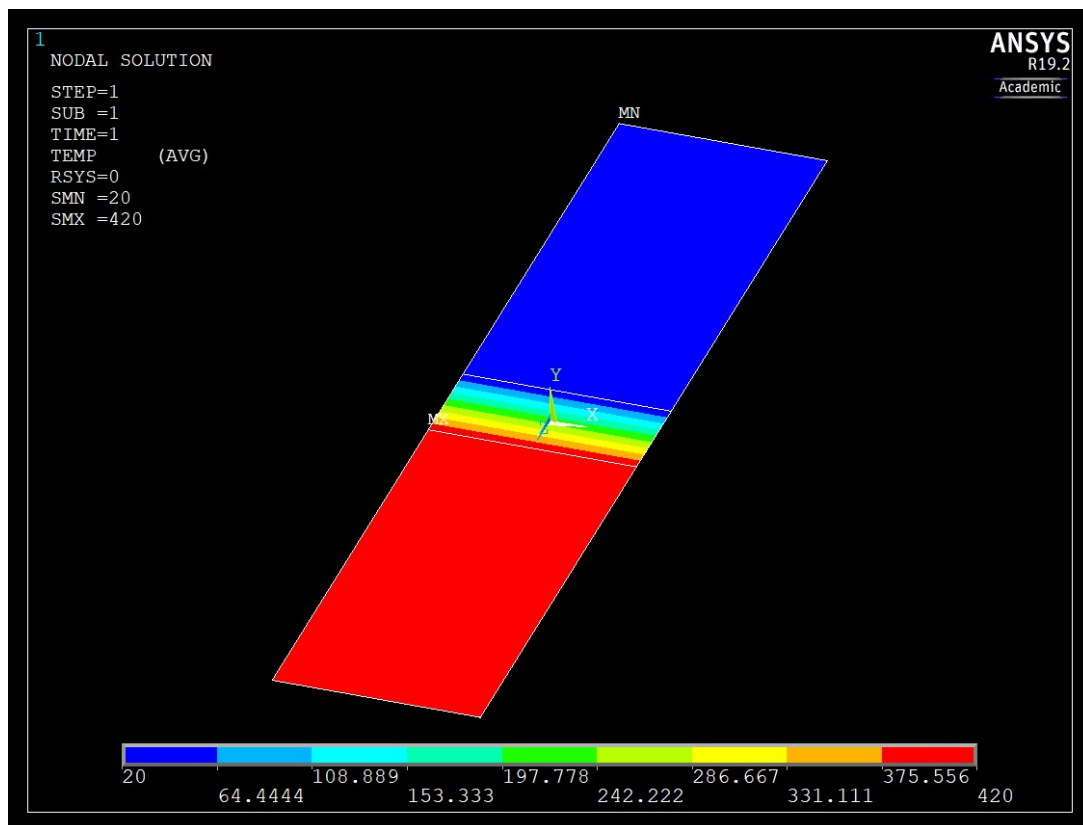


Figure 3.4 – Homogeneous temperature profile.

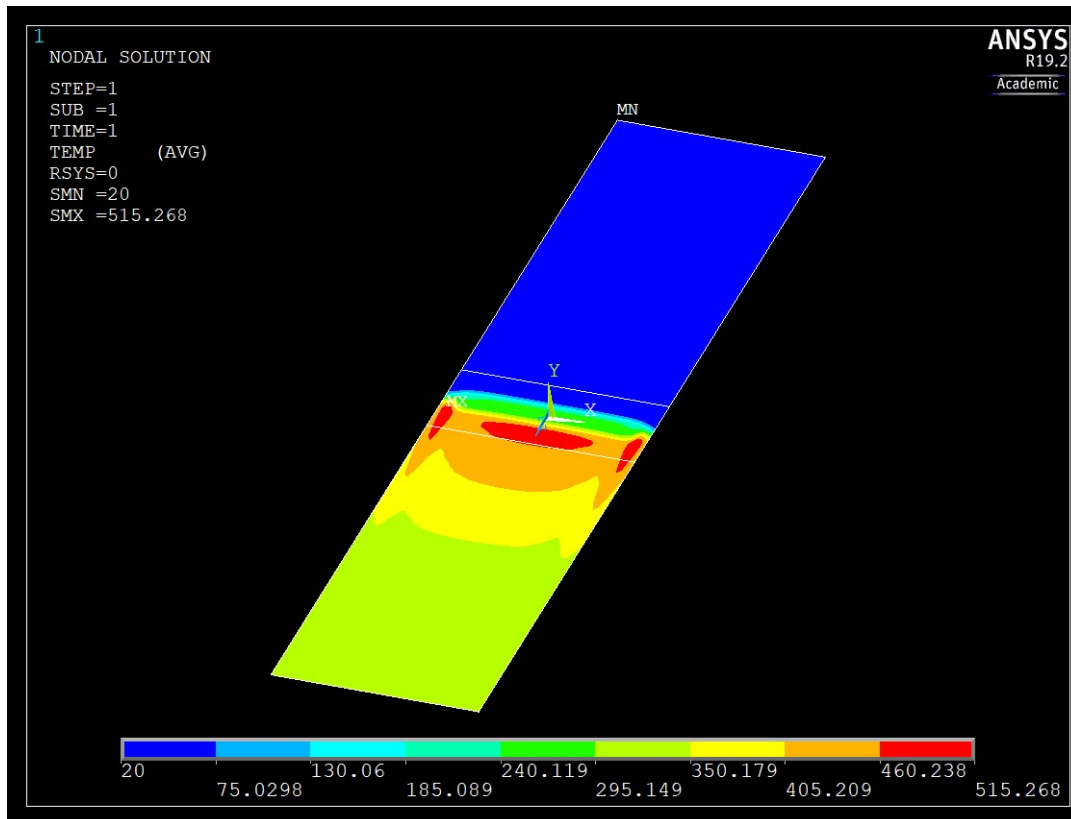


Figure 3.5 – Inhomogeneous/Interpolated temperature profile.

Afterwards, the third part was modified in order to get a more realistic temperature field than the homogeneous heating. The new profile comes from a previous Multiphysics analysis (EM and thermal). The results of this combined analysis are read and then interpolated; the interpolation happens to be a powerful tool as it allows to adapt the new temperature profile to any meshing. This feature makes it possible to recall the same profile even if the mesh of the new model is changed.

On the other hand, the interpolation is the most time-consuming operation of the whole model.

It is possible to explore different temperature fields, in terms of absolute value, using this second initial condition as well; the interpolated temperature profile can be scaled of a certain factor.

The two temperature profiles used are displayed in *Figure 3.4* (homogeneous heating) and *Figure 3.5* (inhomogeneous heating / interpolated profile).

As the thermal stresses for the following structural simulation will be extracted from the temperature profile, the better the latter simulates the real conditions, the more accurate the simulation will be. The temperature gradient map can be an useful qualitative way to evaluate the temperature field; it would be expected to find a greater gradient that follows the geometry of the inductor coil. In the studied case an inductor with rounded shaped corners was simulated and the geometry can be easily noticed in the thermal gradient picture shown in *Figure 3.7*.

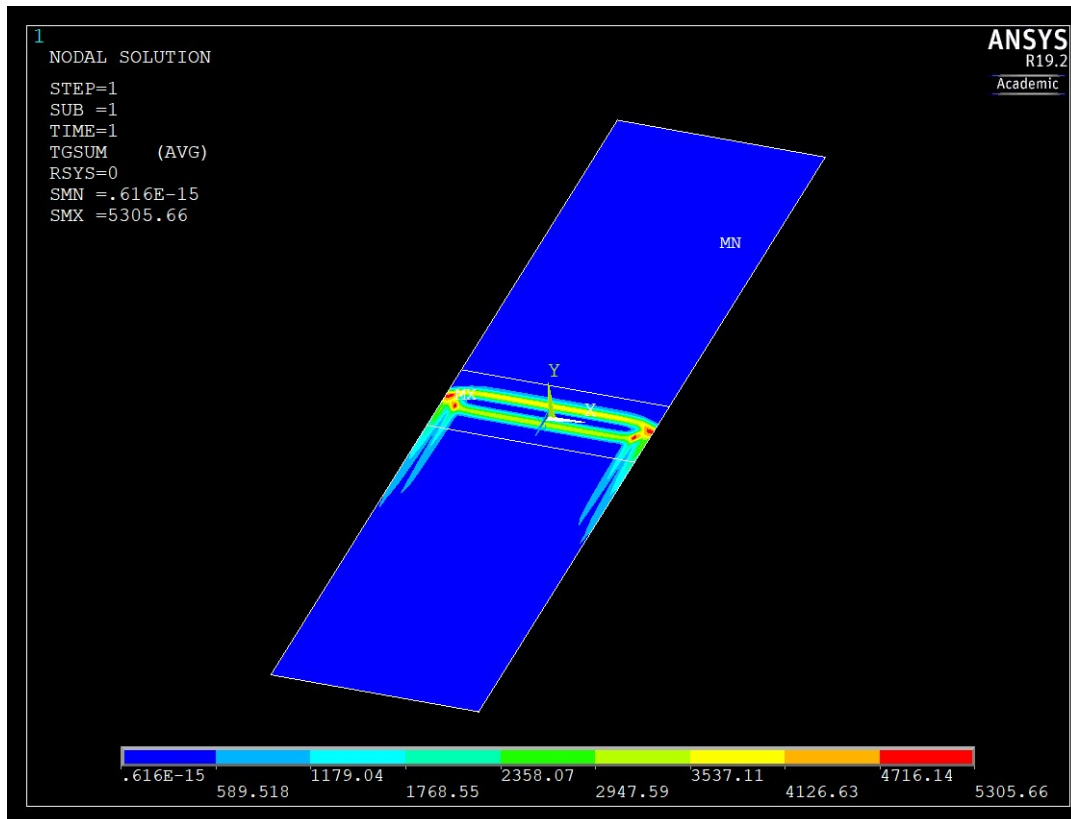


Figure 3.6 – Thermal gradient map for the interpolated temperature field.

The thermal environment code is presented below, divided in the three parts discussed before.

1. Recalling of input data, geometry, meshing and material properties.

```

/FILNAME, WHHH, 1
/config, nres, 50000
/PMETH, OFF
boptn, numb, off

/input, input_data, dat, subprog_input, , 1
/input, geometry_therm, dat, subprog, , 1
/input, attributes_therm, dat, subprog, , 1
/input, mesh_therm, dat, subprog, , 1
/input, prop_therm_1, dat, property, , 1

finish

```

2. Definition of the ANSYS® analysis type.

```

/solu
esel, all
nselect, all
antype, trans
toffset, 273
cnvtol, heat, 1
kbc, 1
trnopt, full
autots, on
esel, all
nselect, all

```

3. Definition of the temperature profile.

```

/assign,rst,WHHH,rth
/solu
  antype,trans

! Homogeneous heating along the 'z' axis implementation
esel,s,mat,,202
nsle
nsel,r,loc,x,x1-eps,x1+eps
nsel,r,loc,y,y0-eps,y0+eps

*get,nnt,NODE,0,COUNT
*dim,temp_z,ARRAY,nnt,6
*dim,maszivz,ARRAY,nnt,1
*get,nmin,NODE,0,NUM,MIN

*do,i,1,nnt
  *get,Zcoor,node,nmin,LOC,z
  *set,Zcoord,Zcoor
  *vfill,maszivz(i),DATA,Zcoord
  *get,nmin,NODE,nmin,NXTH
*enddo

  *do,iii,1,nnt
    *set,MMM,maszivz(iii)
    *set,kkk,iii
    *set,jjjj,iii
    *do,jjj,jjjj,nnt
      *if,MMM,gt,maszivz(jjj),then
        *set,MMM,maszivz(jjj)
        *set,kkk,jjj
      *endif
    *enddo
    ! JJJ
    *set,maszivz(kkk),maszivz(iii)
    *set,maszivz(iii),MMM

    *set,temp_z(iii,1),maszivz(iii)

  *enddo

delT=(tout-tin)/(nnt-1)

*do,iii,1,nnt
  TTT=tin+delT*(iii-1)
  *set,temp_z(iii,2),TTT
*enddo

*do,iii,1,nnt
  nsel,s,loc,z,temp_z(iii,1)-eps,temp_z(iii,1)+eps
  d,all,temp,temp_z(iii,2)
*enddo

```



```

esel,s,mat,,201
nsle
d,all,temp,tin

!esel,s,mat,,202
!nsle
!d,all,temp,200

esel,s,mat,,203
nsle
d,all,temp,tout

esel,all
nsel,all

timestep=1
time,timestep

solve

finish

```

The code regarding the interpolation can be found in the Appendix.

3.3.2 Structural environment

The structural environment is the set of mechanical constraints and boundary conditions that were applied to the model. The simulation of the movement and the behavior of a strip which, in real applications, can both be simply supported by rolls or pulled through the induction heating machine, it is not easy to be represented with the numerical model.

The approach was to keep the structure as “free” as possible. The reason behind this decision is to try to simulate an extreme case, wherein the strip could buckle and deform more easily than in a possibly more constrained application.

For this reason, the mechanical constrains are the following:

- The cold end of the strip is completely fixed (in 3 directions).
- The hot end of the strip is simply supported in the normal direction.

In order to simulate the pulling of the strip, due - for instance - to a continuous process with coils at the end, in further simulations a force was applied in order to put tension in the strip. The results of this test will be later discussed in the parametrical analysis section.

The codification of the mechanical constrains is rather simple and it can be seen in the following fragment of code; it presents both the boundary constraints as well as the applied force. The latter will be applied to one end of the strip while the other remains fixed like it was before.

```

/config,nres,50000
/PMETH,OFF
boptn,numb,off
/input,input_data,dat,subprog_input,,1
/input,geometry_stress,dat,subprog,,1
/input,attributes_stress,dat,subprog,,1
/input,mesh_stress,dat,subprog,,1
/input,prop_stress,dat,property,,1

/PREP7

allsel,all

! Three direction constraining of the cold edge of the strip.
ksel,s,,,1
ksel,a,,,8
lslk,s,1
nsl1,s,1
d,all,ux
d,all,uy
d,all,uz

! 'y' direction constraining of the hot edge of the strip and applied
force application on the same spot.
ksel,s,,,4
ksel,a,,,5
lslk,s,1
nsl1,s,1
d,all,uy
f,all,fz,1

finish

```

The benchmark constraints configuration is displayed in *Figure 3.7*.

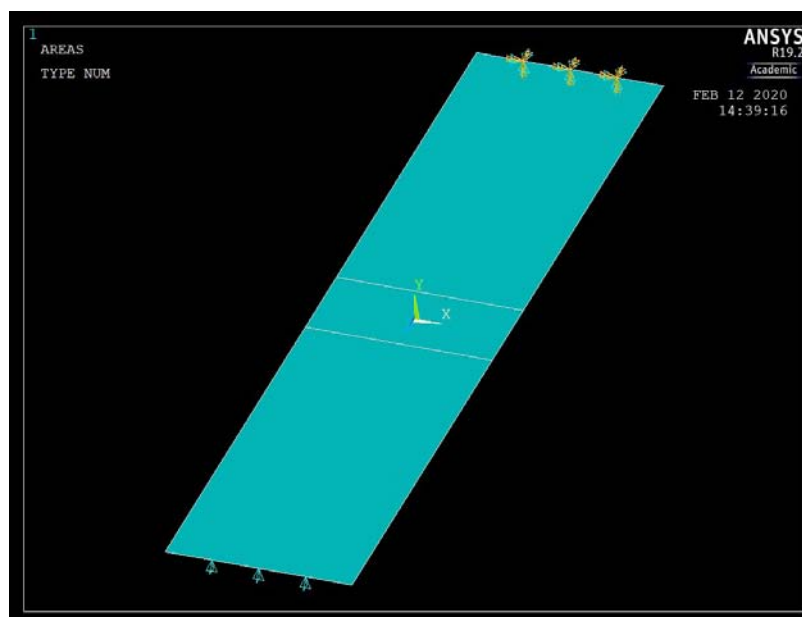


Figure 3.7 – Constraints scheme.

3.4 Model Meshing

A mapped mesh was implemented in the model; the dimensions of the meshing elements are given as input data:

```

nx1=57
  nx1n=1

nz1=60
  nz1n=0.25
nz2=29
  nz2n=1
nz3=60
  nz3n=4.25

```

The $nx1$ parameters sets the number of divisions in the 'x' direction, at the same time $nz1$, $nz2$ and $nz3$ do the same in the 'z' direction and they are respectively referred to areas 201, 202 and 203 (see §3.2.1 for areas definitions). The second parameter ($nx1n$, $nz1n$, $nz2n$, $nz3n$) sets the homogeneity of the mesh, whereas a value equal to one corresponds to an homogeneous mesh while having numbers smaller or greater than one creates a progressive mesh. By progressive it means that the meshing texture becomes finer towards one end of the investigated areas. In the studied case, the two external areas present meshing elements that get smaller towards the central areas which is characterized by a fine mesh itself.

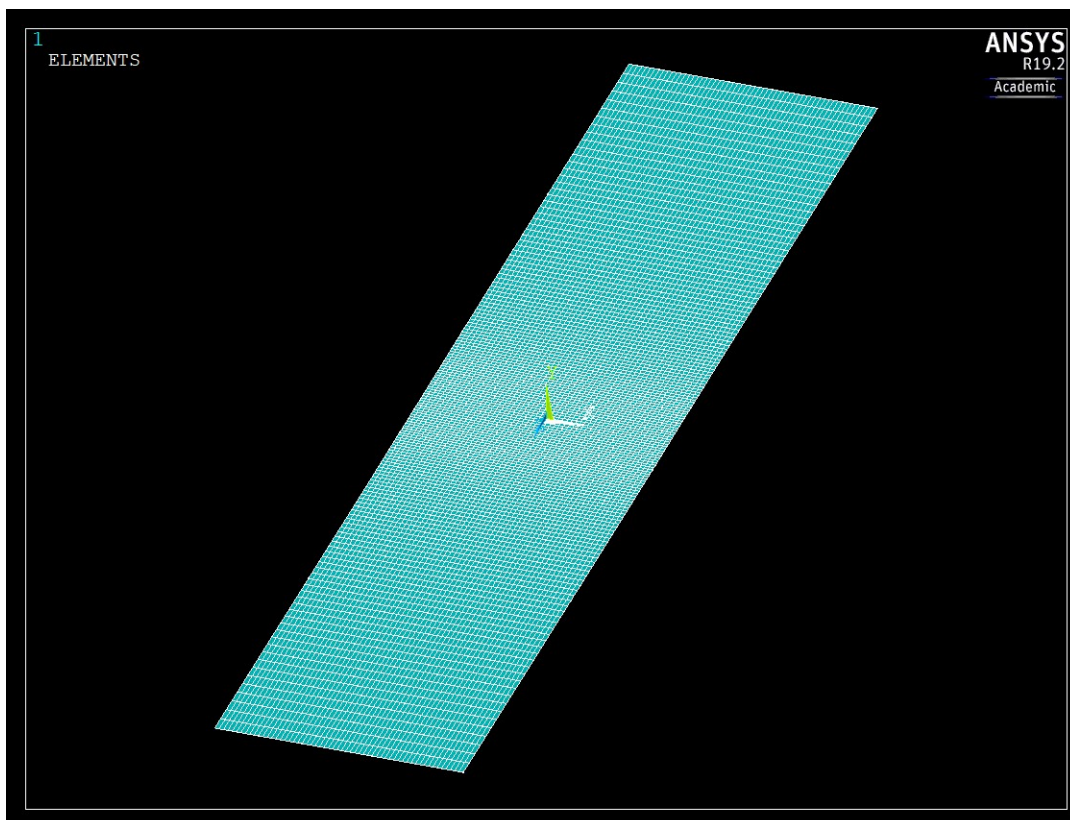


Figure 3.8 – Progressive mesh.

Various meshing textures were tested in order to check the model stability as well as to reduce the computational cost. This process goal was to reduce the number of the mesh elements, firstly by increasing the texture dimensions and, secondly, by introducing the progressive mesh previously explained.

The final choice was to use the progressive mapped mesh. In this way a greater attention is set upon the central section of the strip, as it is the most important because it represents the heating zone. It is the heating zone where, indeed, the biggest temperature field variations should be concentrated. The latter happens to be true within the studied model temperature gradients distribution as well (see *Figure 3.6*). The outcome of the progressive mesh can be seen in *Figure 3.8*.

3.4.1 Model validation through mesh variation

Different dimensions of the meshing elements have been tested; it is important that the model gives the same results, within a certain tolerance, with different meshing grades. By studying the effect of different mesh dimensions and textures, the purpose was to check the stability of the outcomes in order to choose the less time-consuming meshing.

The model proved to be stable. Tests were made in two directions: dimension of the mesh elements and homogeneity of the mesh textures. The modification of both these parameters do not affect the results.

The effect of the mesh refinement, both for the homogeneous heating as well as for the inhomogeneous heating, can be seen in *Figure 3.9*. In the figure, m indicates the dimension of the shortest side of one meshing tile. In particular, the smallest meshing elements are placed in the

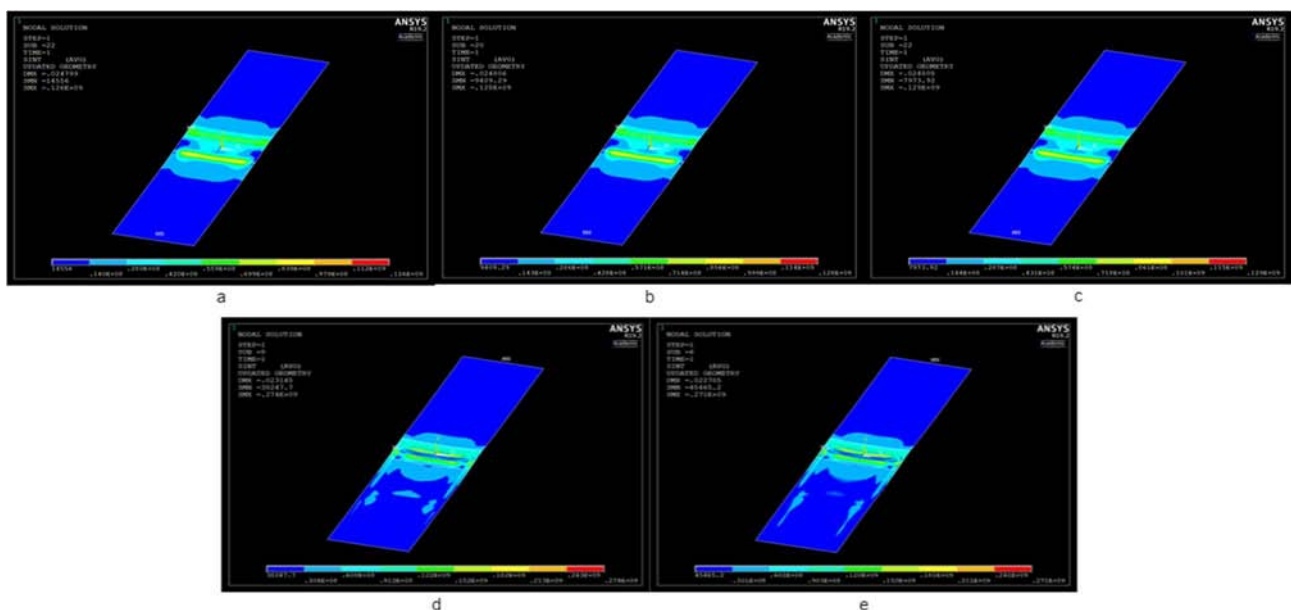


Figure 3.9 – Mesh refinement parametrical analysis. a,b,c) Homogeneous heating; d,e) Inhomogeneous heating. a,d) $m=14\text{mm}$; b,e) $m=7\text{mm}$; c) $m=5\text{mm}$.

central heating zone. As far as it concerns the mesh homogeneity, there is no relevant differences, in terms of outcomes, between using a progressive or a homogeneous mesh. Yet, the homogeneous mesh could become definitely more time-consuming while dealing with small elements.

3.5 Main Settings: number of buckling modes and geometrical factor

The model presents a big number of settings to operate with. Two of them were identified as the most important independent ones as they can deeply influence the results: the number of buckling modes and the geometrical factor (for the geometry updating)

The first one controls the number of buckling modes to be calculated and extracted. Different numbers of buckling modes give different distributions on the stress, as well as different maximum stress and deformation.

In the frame of an ideal procedure, the number of buckling modes should be chosen in order to emulate the real behaviour of any studied workpiece. However, in the case of TFH buckling, the experimental reality is unstable; so, it is not possible to apply this ideal procedure. Instead, the leading idea was to choose a number of modes which allows the strip to buckle rather freely in multiple directions. It was found that three or four buckling modes could be a good compromise.

Commonly, structural linear buckling analyses produce results such as: one or only a few main buckling modes, which are the ones appreciable in reality, plus many negligible ones, which are

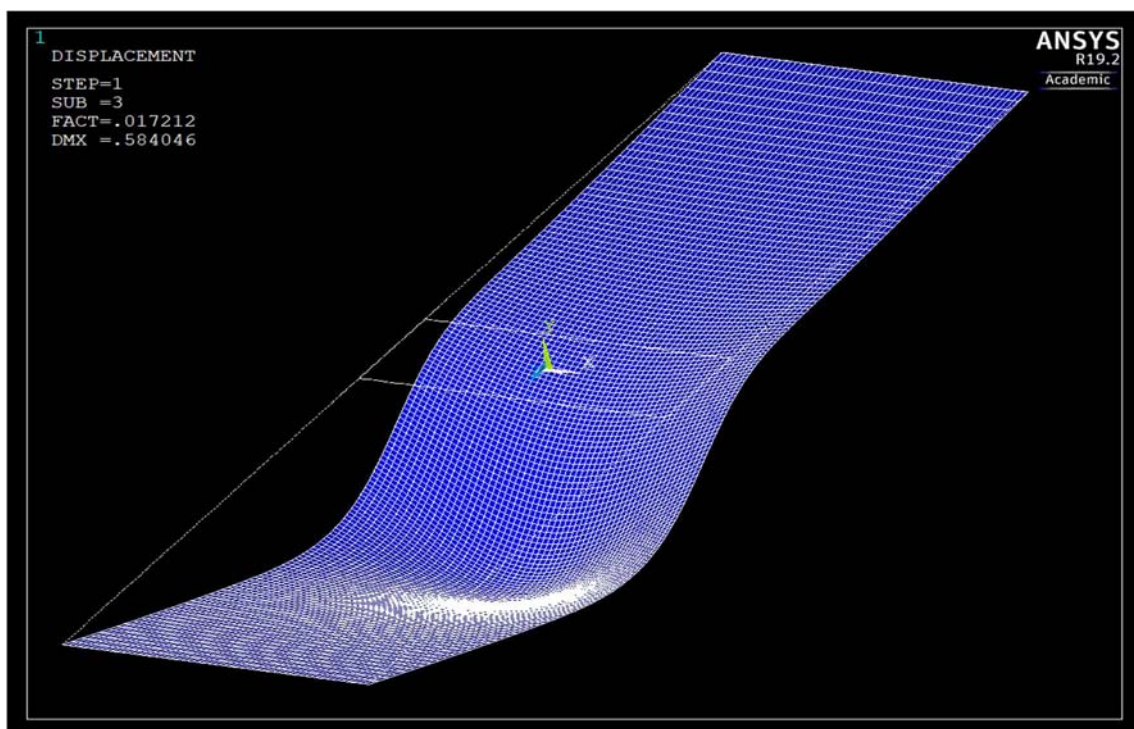


Figure 3.10 – Deformed shape for the linear buckling analysis with 1 buckling mode

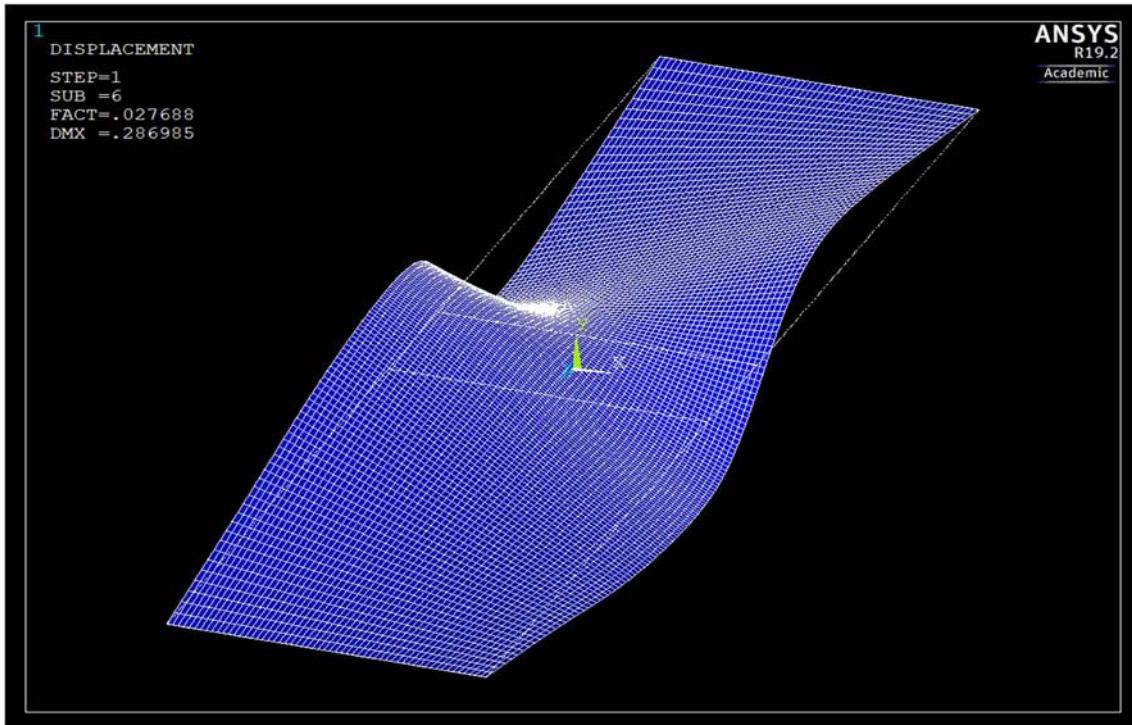


Figure 3.11 - Deformed shape for the linear buckling analysis with 6 buckling modes

more unlikely to occur. For this reason, it is usually recommended, once the number of main buckling mode is found, to extract some more modes.

This way it is possible to check that the identified main mode is really the principal, extracting the others negligible ones will not change the results of the simulation.

As far as this work experience with FEM simulations is concerned, it is unlikely to be true while

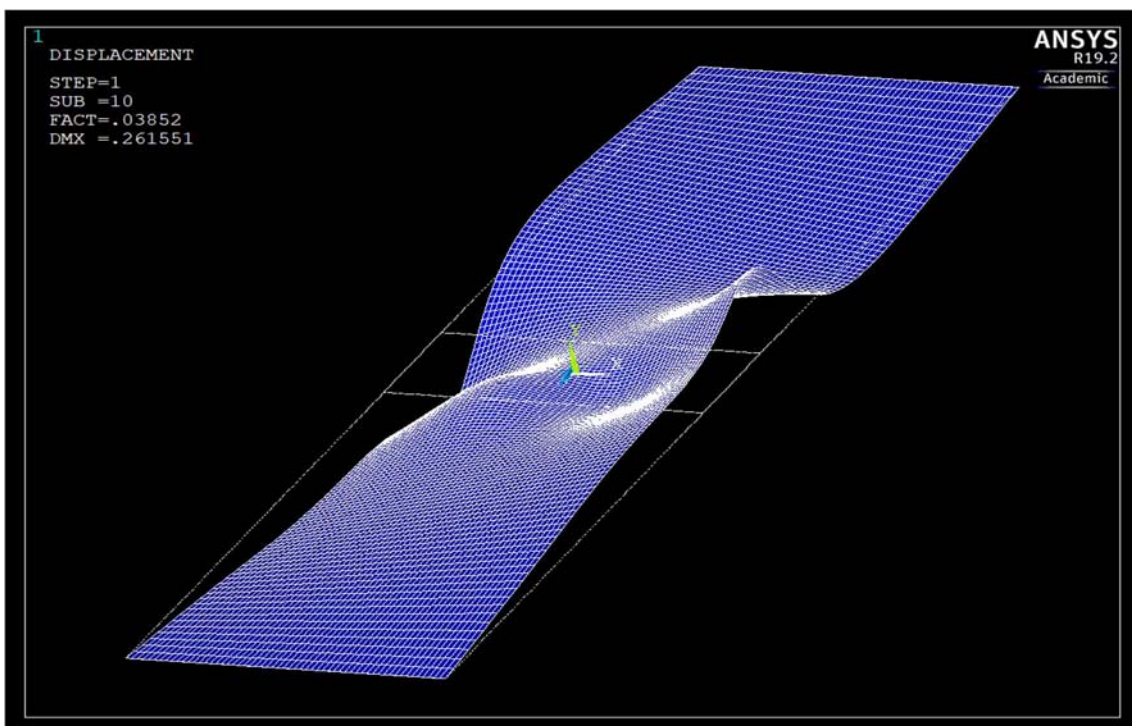


Figure 3.12 - Deformed shape for the linear buckling analysis with 10 buckling modes

dealing with structural loads, but it is no more using thermal loads. In the studied case, by increasing the number of extracted buckling modes, the only appreciable result is a bigger complexity of the solution reached.

The effect upon results of the number of buckling modes can be seen in *Figure 3.10* (one buckling mode), *Figure 3.11* (six buckling modes) and *Figure 3.12* (ten buckling modes).

The second main setting is the choice of the geometrical factor used for the updating of the geometry between the linear and the non-linear buckling analysis. As it was explained in §2.2, the deformed shaped resulting from the linear analysis is used as initial condition for the non-linear analysis. This starting deformation is only qualitative, so it is necessary to set a maximum value of deformation in order to scale the problem.

It is important to introduce this kind of imperfection in the model in order to get the buckling. But if the initial deformation is too big, the result is no more realistic or neither reliable. On the other hand, if the chosen value is too small the non-linear buckling analysis does not work properly, or it does not work at all.

The effect of the geometrical factor is displayed in *Figure 3.13*. The command in the code ('Solving Script' in Appendix) is UPGEOM and the following numerical input is the value of the maximum deformation in meters.

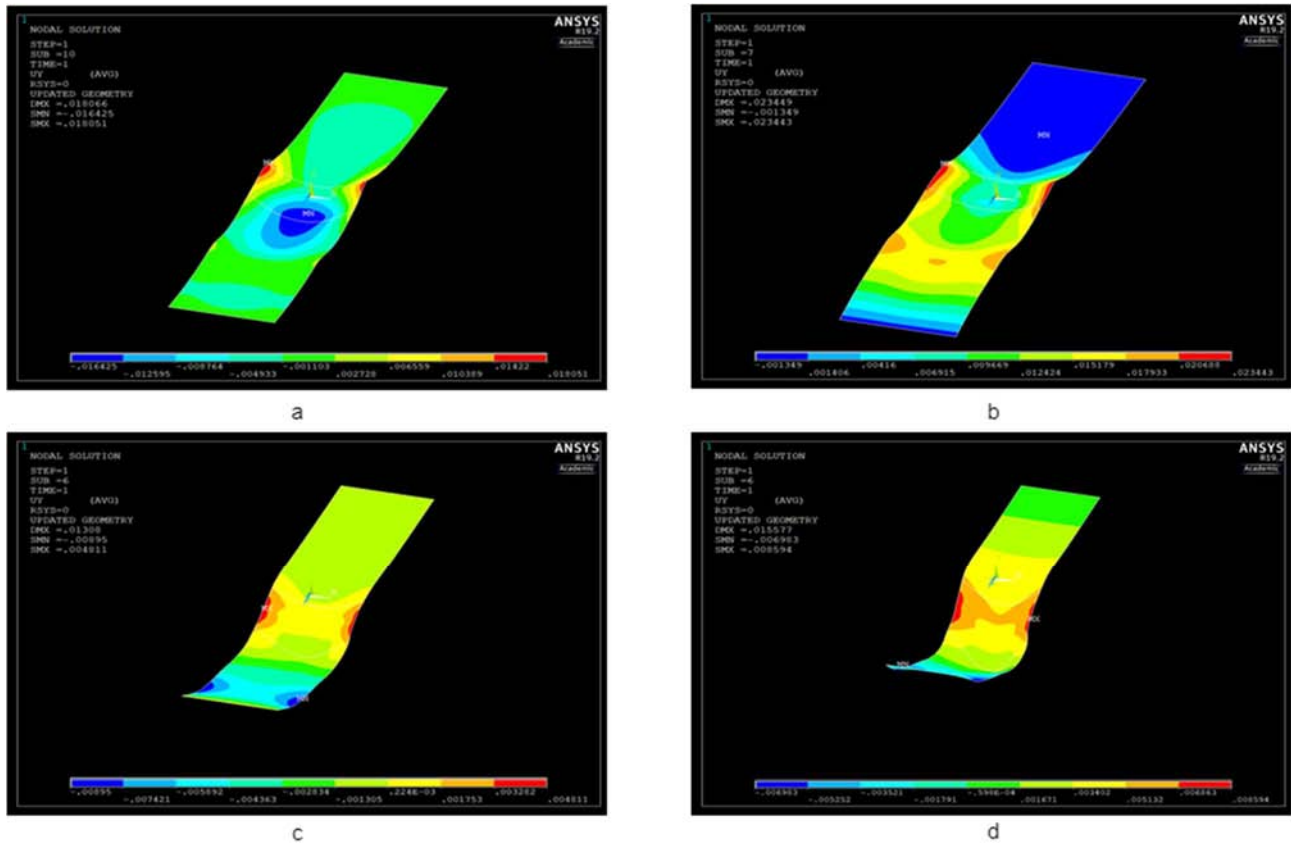


Figure 3.13 – UPGEOM factor effect upon deformation and stress intensity field. a) UPGEOM = 0.01; b) UPGEOM = 0.1; c) UPGEOM = 1; d) UPGEOM = 2;

4 Parametrical Analysis

The phenomenon of buckling is not easy to study or evaluate, as it can depend on a large number of different factors. The main purpose, in the parametrical analysis of the model, was to check if the program reacts properly to any change of boundary conditions and/or input data.

In order to accomplish the goals of this work, the variation of the following parameters has been studied:

- Length of the strip
- Applied force
- Mechanical constraints
- Material properties
- Temperature
- Thickness

All these parameters were firstly analyzed for the homogeneous heating case and later for the interpolated temperature field. Overall, the two cases gave similar results. The main considered

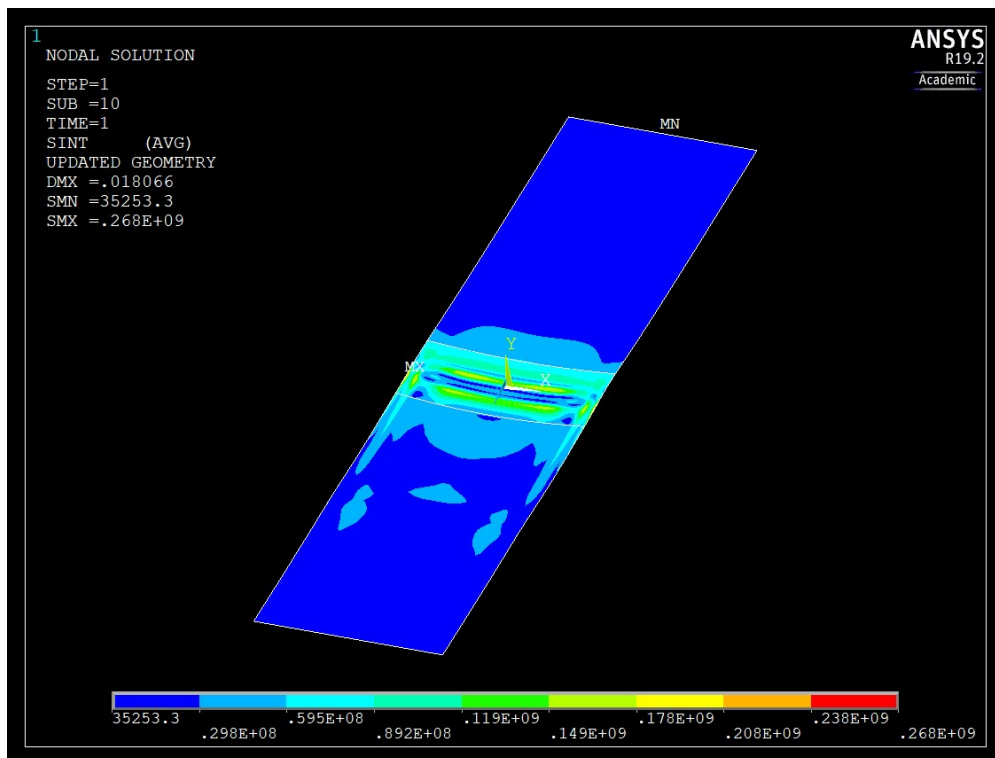


Figure 4.1 – Stress intensity distribution.

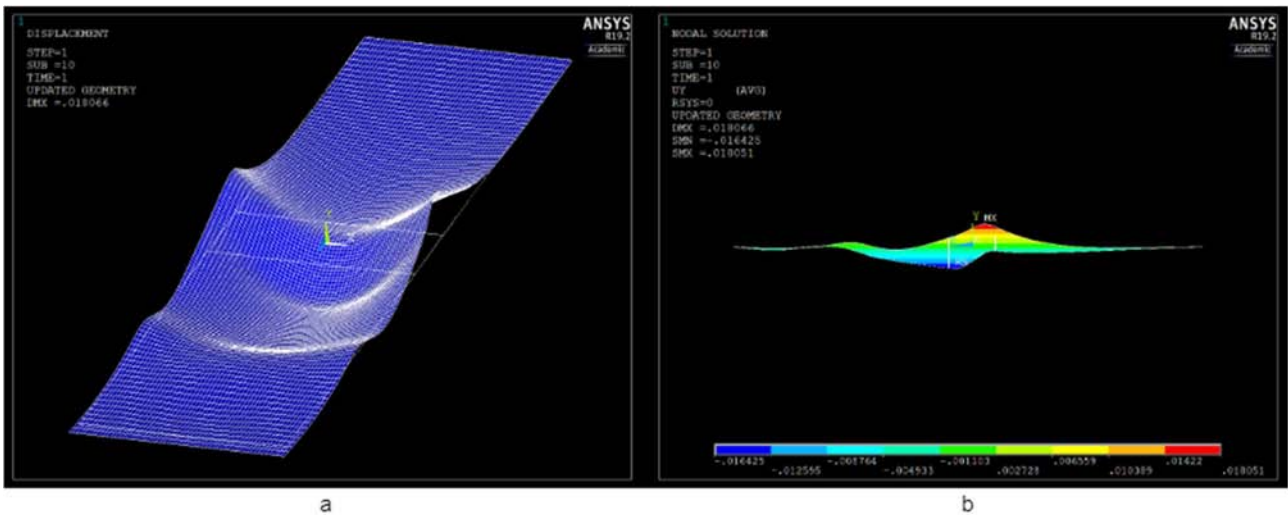


Figure 4.2 – Strip deformed shaped (a) and y-direction displacements (b).

outcomes are the stress intensity distribution and the displacement perpendicular to the motion direction of the strip. The first one is important in order to quantify the stresses that can cause buckling, the latter is the most important displacement to control. In a transverse flux heating configuration, the gap between the inductor and the workpiece can be little and it is a critical parameter in the coupling between the two. Any displacement that alters the distance between inductor and workpiece might have risky drawbacks; by modifying the air-gap the specific power can change as well, changing the temperature distribution alongside with it. Furthermore, if the displacement is too big, it is possible that the inductor and the strip get in contact. This event can cause a discharge in the workpiece that can lead to the interruption of the process and the discard of the workpiece as well. See *Figure 4.1* and *Figure 4.2* for stress intensity distribution and y-direction displacements respectively. These figures could be considered as the benchmark results.

4.1 Length Parameter

Starting from the benchmark length of the strip (2,5 times the width), it was increased to 5 times the width. The main aim in doing so was to check if the behaviour of the strip remains coherent: both in terms of the qualitative stress intensity distribution and in terms of the maximum stress value.

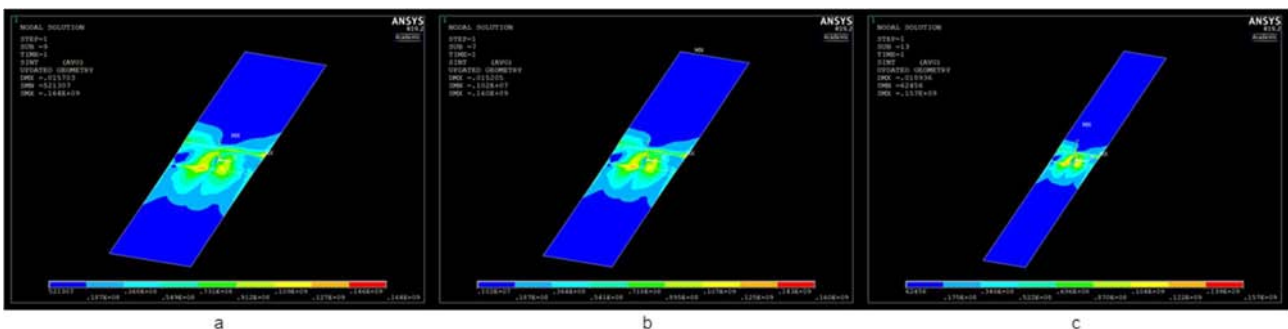


Figure 4.3 – Length variation parametrical analysis, homogeneous heating case. a) Length = $2.5*b$; b) Length = $3*b$; c) Length = $5*b$.

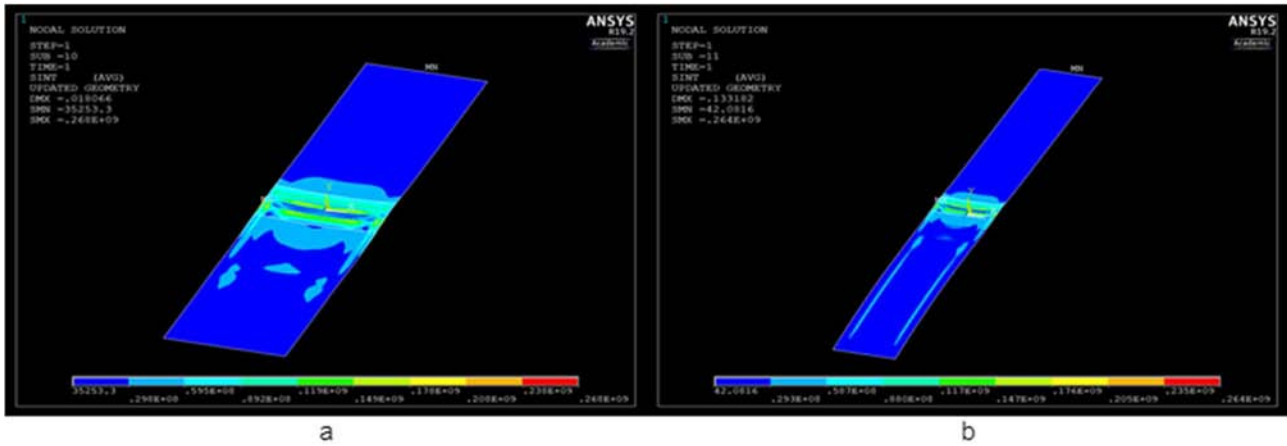


Figure 4.4 – Length variation parametrical analysis, inhomogeneous heating case. a) Length = $2.5*b$; c) Length = $5*b$.

The model proved to be stable as it does not present big qualitative/quantitative differences between the different lengths tested. Furthermore, the most important aspect is that the biggest stress intensity remains in the central part of the strip and does not move towards the ends. It could be a sign that the mechanical restrains are not affecting the results.

Even though the non-homogeneous heating shows a little difference passing to a longer strip, the result can be still considered stable. The results of the homogeneous and inhomogeneous heating case are displayed, respectively, in *Figure 4.3* and *Figure 4.4*.

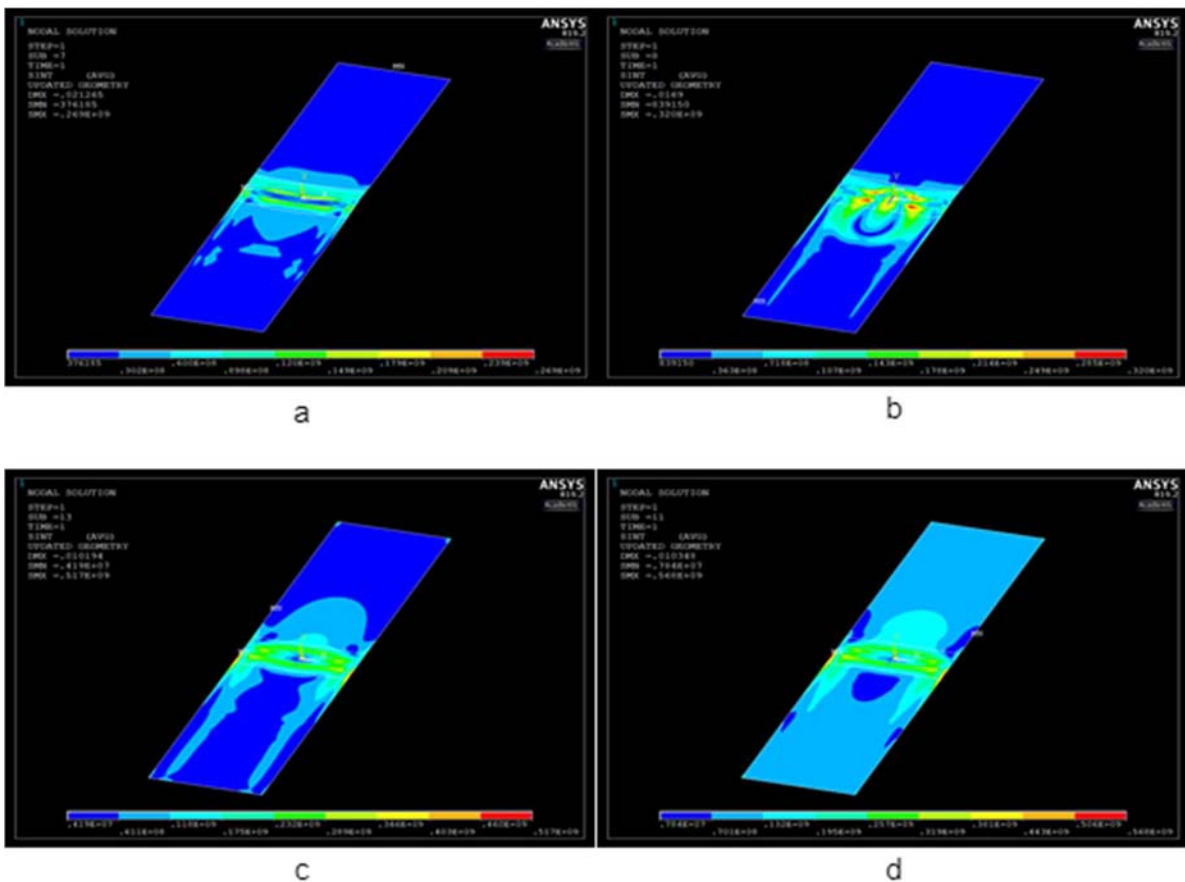


Figure 4.5 – Applied force variation parametrical analysis. a) $F=10N$; b) $F=300N$; c) $F=850N$; d) $F=2000N$.

4.2 Applied Force Parameter

In order to simulate the behaviour of the metal strip in a real transverse flux induction heating process, the workpiece must be set in tension. This is what commonly happens in a line process where the strip is pulled through different process stations.

The model, both in the homogeneous and in the non-homogeneous case, reacts to the variations of the amount of force applied.

The force is applied at the hot end of the strip to the whole ending section. By increasing the value of the force, different stress distributions and intensity are achieved. In particular, it is possible to notice that after a certain amount the stress distribution starts to interest all the strip and not only the heating zone. A possible interpretation of this phenomenon could be that the homogeneous tension applied to the whole strip becomes more relevant than the stresses caused by the buckling phenomenon. *Figure 4.5* shows the effect of an increasing applied force upon the stress intensity distribution.

4.3 Mechanical Constraints Parameter

The modification of the mechanical constraints proved to be a delicate parameter to deal with. The model works well with the standard configuration, presented in §3.3.2. Only a few other configurations proved to work.

One other constraints test was carried, it concerned the possibility of fixing a portion of the strip and not only the ending sections. By “fixing” it means preventing a portion of material to move in the orthogonal direction. It can work as a simulation of the clamping of the workpiece.

The results show that the stress intensity increases by increasing the fixed zone; this is an expected

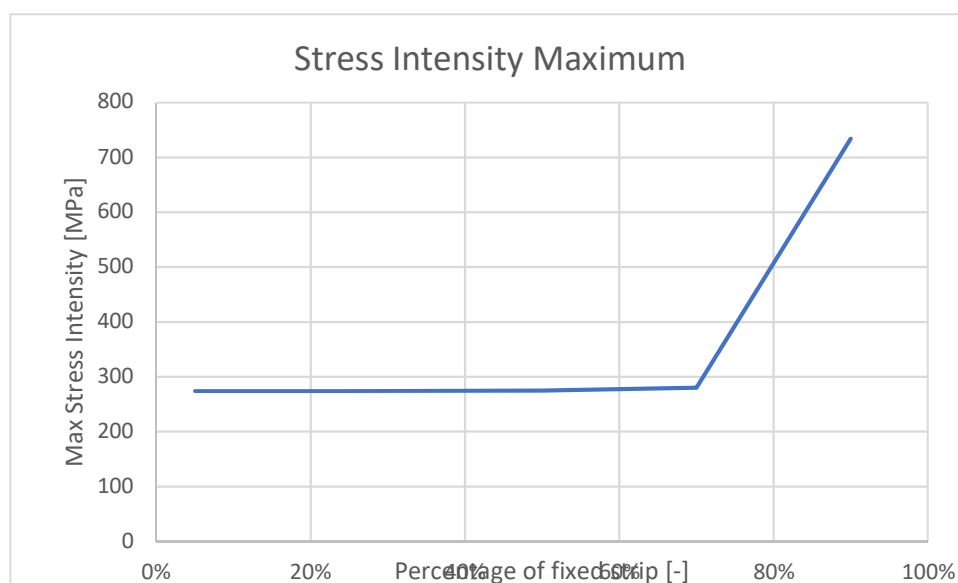


Figure 4.6 – Maximum stress intensity over percentage of strip fixed.

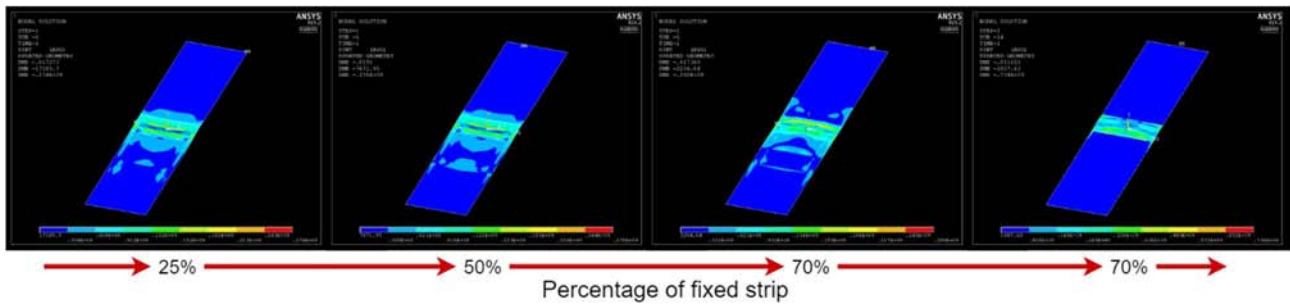


Figure 4.7 – Variation of the stress intensity distribution according to the percentage of fixed strip.

effect because, by adding stronger constraints the strip stiffness should increase consequently. The effect upon the stress intensity distribution is not evident until really wide fixed zone (70% - 90%). The stress intensity maximum absolute value is stable until big percentages of strip fixed. It can be interpreted as an irrelevance of this kind of constrains, that can be said because high percentages of fixing are unrealistic. The evolution of the stress intensity distribution can be seen in *Figure 4.7*.

4.4 Material Properties Parameter

In this section, the effect of different material properties upon the model has been investigated. This investigation developed in two directions: testing different materials as well as testing the introduction of more temperature dependent properties. Talking about the latter, in the first phase only temperature dependent conductivity and specific heat were used. In a second phase also temperature dependent elastic modulus and coefficient of thermal expansion were implemented.

The results are straightforward: the model easily adapts to these different inputs giving results which coherently change with the different tested material.

During the initial phase, the homogeneous heating simulation, generic steel properties were used. They are collected in *Table 4.1* and *Figure 4.8*.

Material Property	Value
<i>Young's Modulus</i>	<i>2 GPa</i>
<i>Poisson's Ratio</i>	<i>0.3</i>
<i>Density</i>	<i>7800 kg/m³</i>
<i>Coefficient of Thermal Expansion</i>	<i>11.9·10⁻⁶ 1/°C</i>

Table 4.1 – Material properties of generic steel.

In order to get a better comparison between the homogeneous heating simulation and the non-homogeneous one, the same properties were used in both cases. Once the interpolated, non-homogeneous temperature field proved to give reasonable results, the material properties of the stainless steel, previously used in an experimental setup, were implemented. This choice was taken in order to set the possibility of future comparisons between the numerical results and experimental

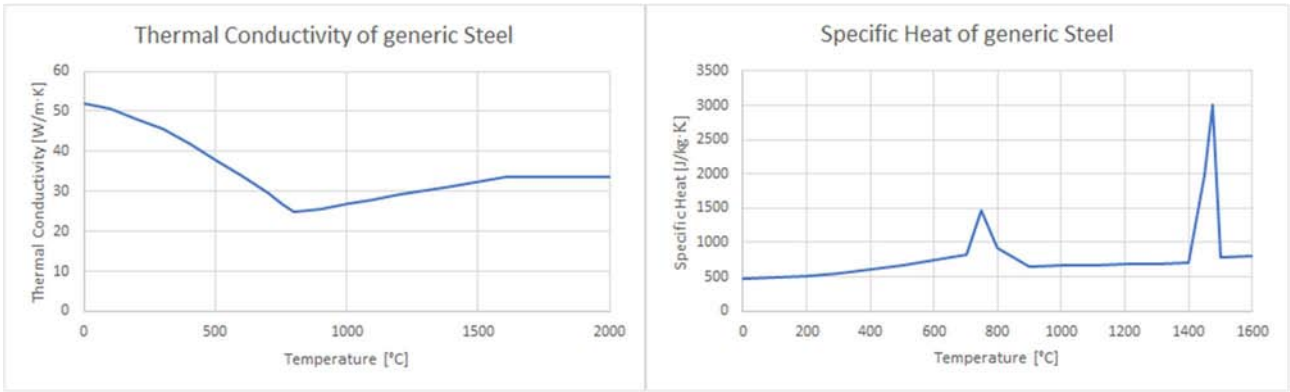


Figure 4.9 – Charts of thermal conductivity and specific heat of a generic steel.

evidences.

The chemical composition and the material properties of this stainless steel are shown in Table 4.2, Table 4.3 and Figure 4.9.

Element	Percentage
<i>C</i>	0.05%
<i>Cr</i>	14.0%
<i>Ni</i>	7.0%
<i>Cu</i>	0.7%
<i>Ti</i>	0.4%

Table 4.2 – Stainless Steel composition.

Material Property	Value
<i>Young's Modulus at 20°C</i>	2.00 GPa
<i>Young's Modulus at 200°C</i>	1.88 GPa
<i>Specific Heat</i>	500 J/kg·K
<i>Poisson's Ratio</i>	0.30
<i>Density</i>	7760 kg/m ³

Table 4.3 – Material Properties of the Stainless Steel.

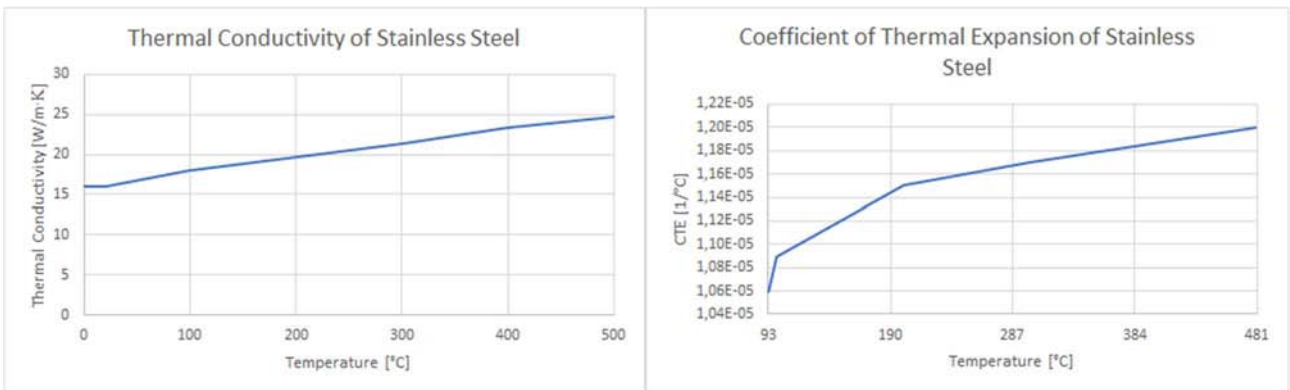


Figure 4.8 – Charts of Stainless Steel thermal conductivity and coefficient of thermal expansion.

4.5 Temperature Parameter

The effect of temperature upon the buckling behaviour was analysed both for the homogeneous heating as well as for the interpolated temperature field. In the first case the low temperature was fixed and equal to room temperature, while the final temperature has been increased. In the second case the totality of the temperature profile has been scaled of a certain factor. The model behaves well according to the temperature variation: both the maximum stress intensity and the deformation amplitude increase alongside the temperature.

The meaning of “displacement amplitude” is the maximum distance in the orthogonal direction between the lowest and the highest point of the deformed shape. The displacement amplitude is displayed in *Figure 4.10*, it corresponds to the value of the distance between the points marked as MX and MN.

Concerning the results, it is necessary to point out that both the behaviours of stresses and displacements are coherent with the increase of temperature. Towards the lowest temperatures it seems the model tends to a critical value both concerning stresses and displacements. A possible explanation of this phenomenon is that the thermal buckling is not triggered working at low temperatures. So, the critical minimum value of stress can be attributed only to the thermal stresses caused by thermal expansion. The absolute value of those is probably not high enough to cause the

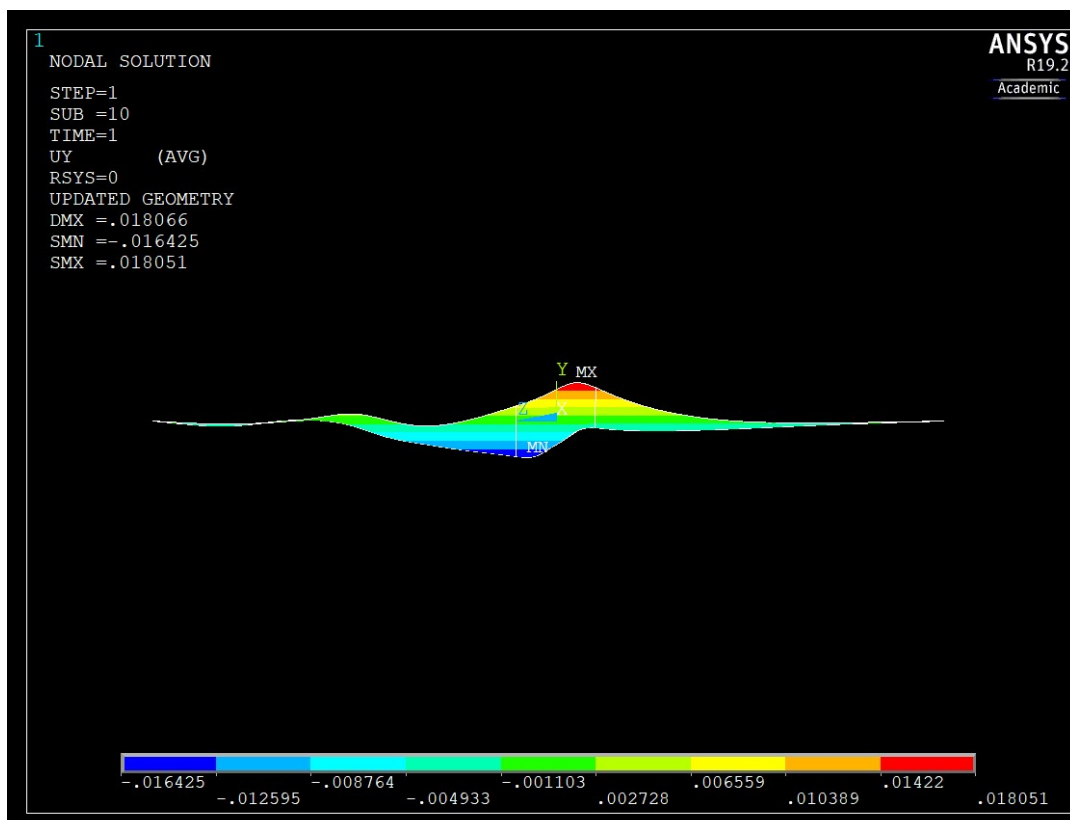


Figure 4.10 – Displacement Amplitude.

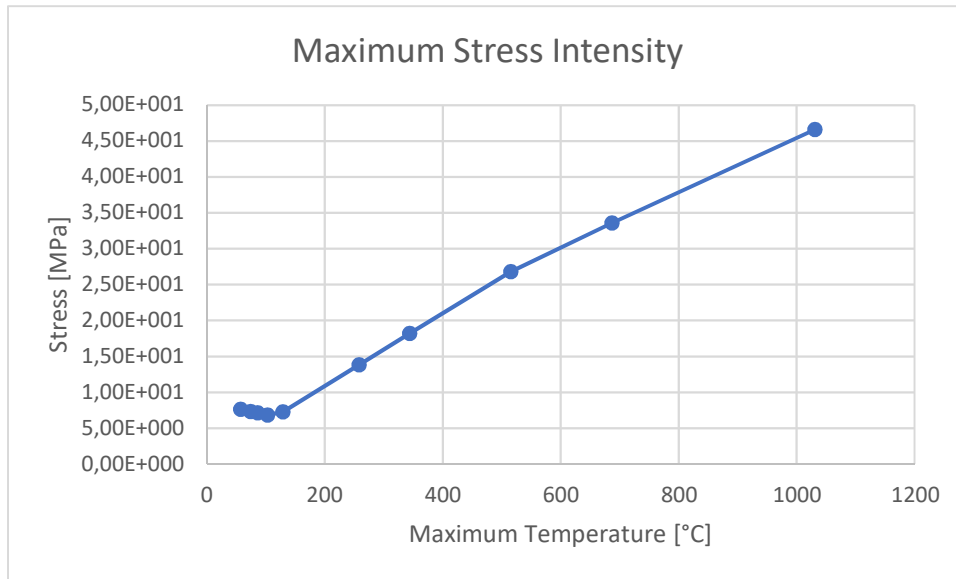
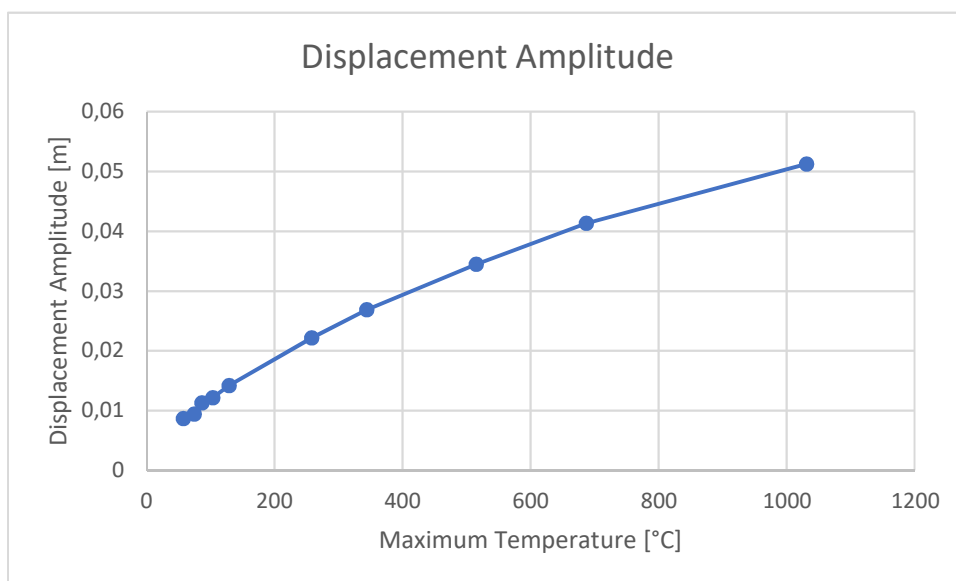


Figure 4.11 – Maximum stress intensity behaviour according to the temperature variation.

buckling; the deformation of the strip, both elastic and/or, in the worst scenario, plastic, caused by the buckling might be the cause of the maximum stress intensity rise once a certain temperature is reached.

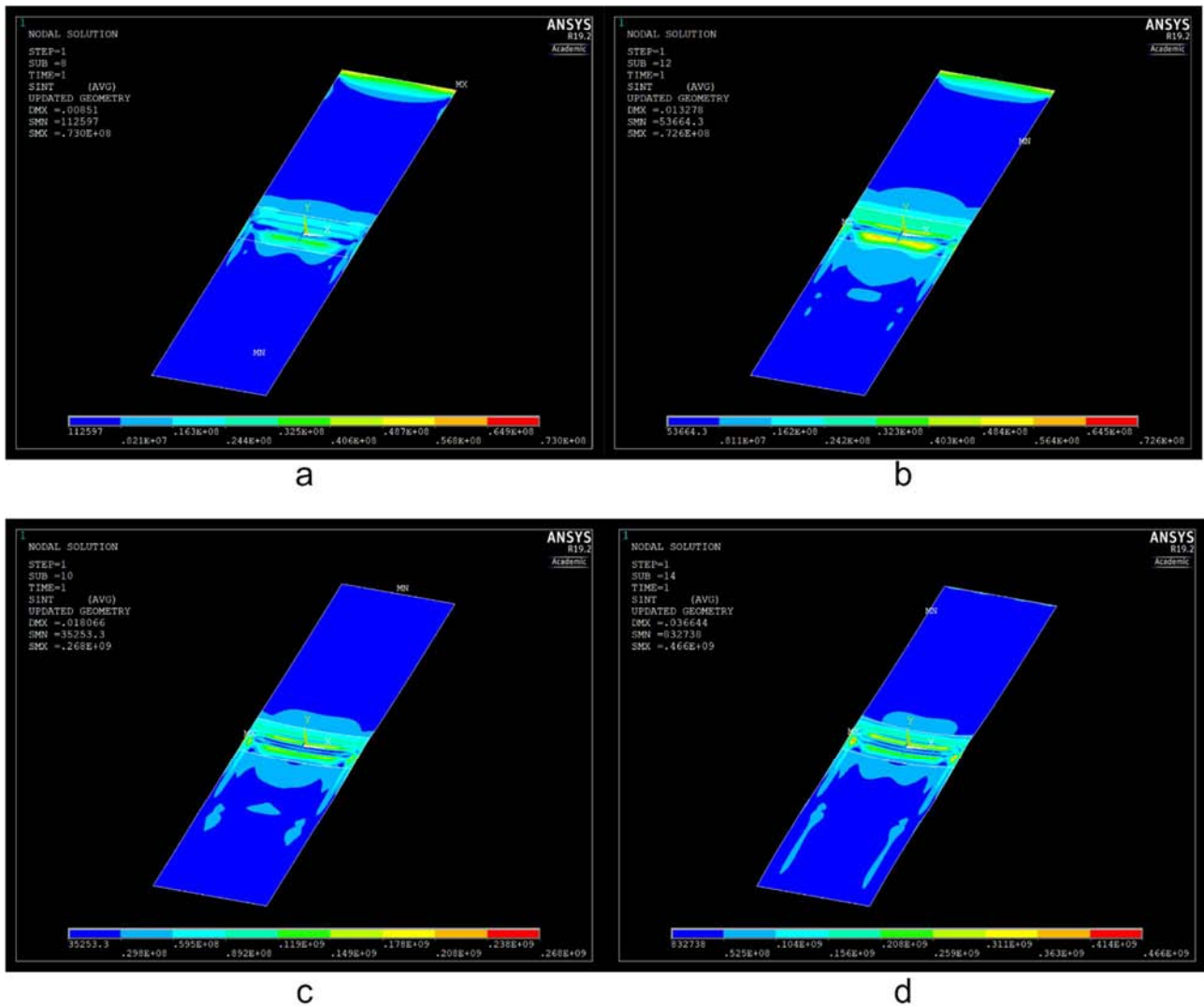
In contrast, concerning the displacement amplitude, the critical value displayed might be due to the initial status of the strip. It is an already deformed shape that comes from geometry update performed after the linear buckling analysis. In particular, the amount of displacement shown by the second graph could depend upon the geometrical factor used. In all these simulations this factor was set to a maximum deformation of 0,01, which is exactly the critical value.

The behaviours of stress intensity and displacement amplitude according to temperature variations are shown respectively in *Figure 4.11* and *Figure 4.12*. In both the charts, each point has been



calculated with a different temperature profile; the value of the temperature taken into account is the

Figure 4.12 – Displacement amplitude behaviour according to the temperature variation



maximum of each profile.

Figure 4.13 – Stress intensity distribution results with different temperature profiles.

Maximum temperatures: a) $\sim 58^{\circ}\text{C}$; b) $\sim 129^{\circ}\text{C}$; c) $\sim 515^{\circ}\text{C}$; d) $\sim 1030^{\circ}\text{C}$.

The qualitative behaviour of the stress intensities is harder to interpret; nonetheless, the results stay consistent in terms of the concentration of the stress that mostly lays in the central portion of the strip, particularly, while dealing with average or high temperatures (c and d in Figure 4.13). These will be the most useful results as those are the temperatures used in real applications. The evolution of the stress intensity according to the temperature variation is displayed in Figure 4.13.

4.6 Thickness Parameter

The relationship between the buckling behaviour and the thickness is the most outstanding. As the graph shows, the displacement amplitude presents a clear buckling/non-buckling separation. It is physically adequate to imagine a major buckling for small thicknesses and an absence (or negligible entity) of buckling for bigger thicknesses. Figure 4.14 clearly shows the switch between buckling

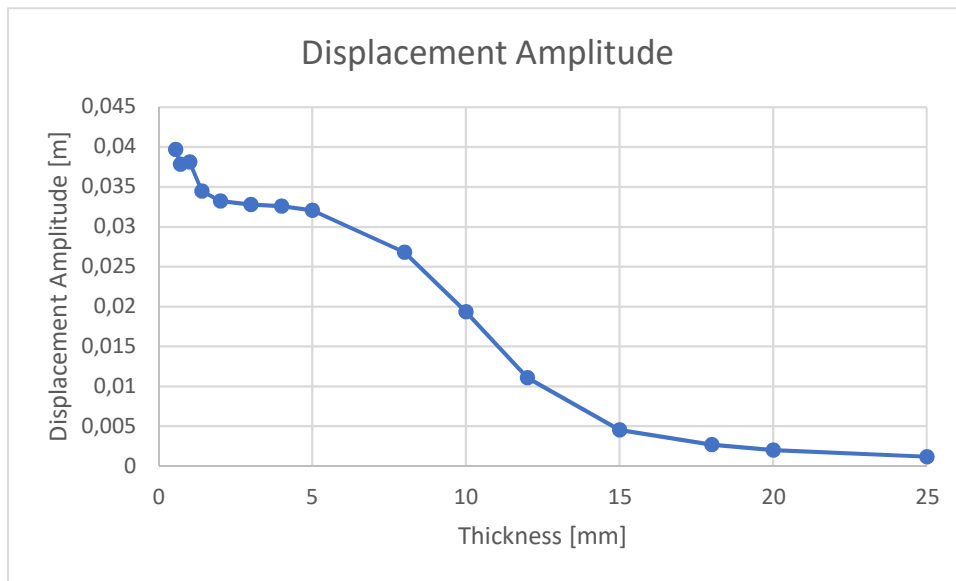


Figure 4.14 – Displacement amplitude behaviour according to the thickness variation.

occurrence and buckling non-occurrence at a thickness value between 5 and 10 millimeters. This value depends upon the geometry and the constraints of each model; it must not be intended as an absolute critical value. In the chart, the small group of values in the top left corner concerns thickness below 1mm. Even though the results follow the trend of the curve, the simulation proves not to be stable for such small thickness.

Conclusions and Perspectives

A numerical model for the buckling analysis concerning the behaviour of a transverse-flux heated strip has been developed. The model proved to be consistent through the various parametrical analyses. Consistency has always been the main goal of this work, so, the achieving of it can be considered as the main outcome.

It is important to point out that this is not a ‘final’ result. The buckling analysis described in this work should be collocated in the bigger frame of a more spread investigation upon the transverse-flux induction heating process. As it stands, the model could also be included in a Multiphysics simulation; keeping as main objective of it the optimization of the TFH process. The possible workflow could be to perform first a coupled electro-magnetic and thermal simulation and then, as it has been done, to use the thermal results as starting point of the buckling analysis. The latter can both work as a final check of a process or, on the other hand, as a goal function in designing operations.

As far as it concerns future developments, there is the possibility of improvements of the model in two directions: a numerical improvement and a non-numerical one. By numerical improvement, it means to further develop the FEM simulation in order to get a more precise and efficient one. The non-numerical developments could be the integrations of the numerical results with experimental evidences.

Numerical Improvement of the Model

The possible further numerical developments of the model could be:

- In terms of applicability, it could be useful to prove the model stability in dealing both with different workpiece geometries as well as with different temperature field geometries.
- The implementation of a ‘buckling goal function’. In this way the simulation procedure will work in the other direction; it would start from a deformed shape or a stress intensity distribution to arrive to the necessary temperature field to obtain them. For instance, it would be interesting to have the possibility to set a certain amount of tolerable out of plane displacement and, starting from it, to calculate the amount of stress that would cause it and then the temperature field responsible of it. Later, a proper inductor which produces that specific temperature field could be designed.
- As it appears clear that the main actor in the buckling occurrence is the inhomogeneity of

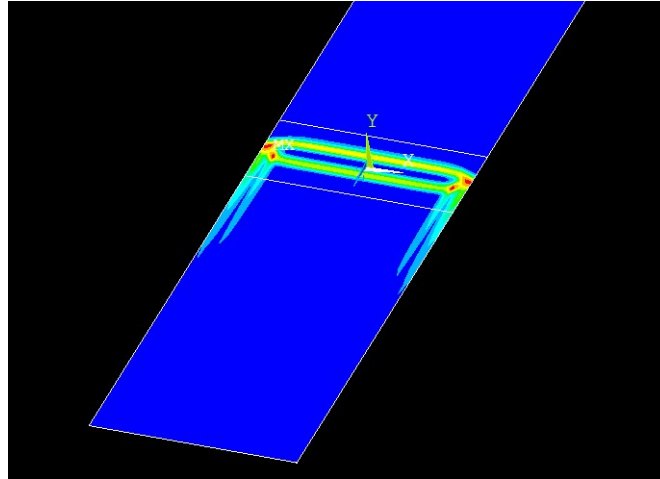


Figure A – Thermal gradient

the temperature profile, the most important aspect to work on is the inductor shape. In particular, it would be useful to develop a changing-shape inductor. The temperature gradient distribution strictly follows the inductor shape (*Figure A*); by changing the geometry it would be possible to adapt the gradient in order to get any desired temperature profile. It would also be possible to adapt the inductor shape to any workpiece shape. This development is surely feasible inside a FEM simulation, in contrast, the feasibility of a real set-up of a moving inductor should be carefully studied.

- In order to further check the consistency of the results of the buckling analysis in ANSYS®, it would be advisable to carry out the same simulation, or a similar one, in other simulation environments.

Non-numerical Developments

As it stands, the simulation discussed in this work is solely numerical. The validation of the numerical results could only be carried out through the integration of them with experimental evidences. In the studied case any measurement would be complicate due to the instability and the temperatures of the real process.

Until now the displacement results have only be compared to an estimation of the real deformation. If it would became possible to get the real value of it, a different simulation could be developed; in this case the imperfection that had to be introduced to perform the non-linear buckling analysis would be the deformed shape (resulting from the linear buckling analysis) no more. It would be possible to introduce it as a geometric imperfection the experimentally measured deformation.

One possible way to deal with the problem of measurements could be to use optical systems.

Another non-numerical development could be the investigation of the effect of the changing of the

mechanical constraints. In a certain measure, the way the strip is moved and constrained must influence the occurrence of buckling. Before performing the change of boundary condition via FEM simulations, the mechanical constraints should be studied and understood in a real experimental set up. In the implemented code presented the constraints have been the main unknown boundary condition. It would be useful to run some experimental test with straightforward configurations. They have to be replicated in the model to validate the numerical results by comparing them with the experimental ones. By straightforward configuration it means to set physical constraints easily transformable in boundary conditions in the code. For instance, a non-moving and completely fixed strip could be used as a benchmark test.

References

1. ANSYS Mechanical APDL®, release 19.2, *Element Reference, 7: Element Library*, Ansys, Inc.
2. ANSYS Mechanical APDL®, release 19.2, *Theory Reference, 11: Shape Functions*, Ansys, Inc.
3. ANSYS Mechanical APDL®, release 19.2, *Theory Reference, 15: Analysis Procedures, 15.5 Buckling Analysis*, Ansys, Inc.
4. ANSYS Mechanical APDL®, release 19.2, *Structural Analysis Guide, 7: Buckling Analysis*, Ansys, Inc.
5. Banichuk N., Jeronen J., Neittaanmäki P., Tuovinen T., *On the instability of an axially moving elastic plate*, International Journal of Solids and Structures, 2010, 47. 91-99.
6. Barglik J., *Induction Heating of Thin Strips in Transverse Flux Magnetic Field*, Advances in Induction and Microwave Heating of Mineral and Organic Materials, 2011, Stanisław Grundas, IntechOpen, DOI: 10.5772/13324.
7. Bartlett Quimby T., *A beginner's Guide to the Steel Construction Manual*, 2017, 15th edition, Chapter 6 – Buckling Concepts.
8. Bianchi N., Dughiero F., *Optimal Design Techniques Applied to Transverse-Flux Induction Heating Systems*, IEEE Transactions on Magnetics, 1995, Vol.31, No.3
9. Bobart G.F., *Technical Note: Transverse Flux Induction Heat Treating*, J. Heat Trea., 1988, New York, 6:47-52.
10. Deshpande S., *Buckling and Post Buckling of Structural Components*, 2010, The University of Texas at Arlington.
11. Hassan, Kurgan, *Modeling and Buckling Analysis of Rectangular Plates in ANSYS*, 11:310-329, 10.24107/IJEAS.531011.
12. Keyes D et al., *Multiphysics simulations: Challenges and opportunities*, 2013, The

- International Journal of High Performance Computing Applications, vol.27, no.1.
13. Luo H., Dunbar W.S., Moore J.E., *Buckling Analysis of a Heated Steel Strip in a Continuous Annealing Furnace*, Journal of Manufacturing Science and Engineering-transactions of The Asme, 1999, 121. 10.1115/1.2830578.
 14. Minen M., Codutti A., Gagliardi N., Petronio M., Guastini F., Ren J-Y., Audeon D., *Development of an high power density transverse flux inductor for the Danieli Universal Endless process*, 2019, HES-19 Heating by Electromagnetic Sources.
 15. Ruhnke A., Mulbahuer A., Nikanorov A., Demidovitch V., *Thermal deformation of the strip during transverse flux induction heating*, COMPEL: The International Journal for Computation and Mathematics in Electrical and Electronic Engineering, 2000, vol 19, p. 730.
 16. Schulze M., Nikanorov A., Nacke B., *Design of Transverse Flux Induction Coils by Using a Successive Optimization Strategy*.
 17. Spagnolo A., *Auto-adaptive multi-coil inductors for transverse flux heating of metal strips*, 2011, Università degli Studi di Padova, Phd Thesis.
 18. Wolfe C., *Multiphysics: The Future of Simulation from Ansys Advantage*, 2014, Ansys Inc., Vol.VIII, Issue 2.
 19. Yang, J., Tang, D., Su, L. et al, *Effect of roller shapes on strip buckling in a continuous annealing furnace*, Int J Miner Metall Mater, 2011, 18, 297–302.

Appendix

Thermal Environment Script

! Resuming the thermal environment

```
resume,environment_therm_1,db
```

```
    /assign,rst,WHHH,rth
```

```
/view,1,8,-7,-3
```

```
/ang,1,-35
```

! Calling the interpolation program

```
/input,out_xyzT_new,dat,Subprog
```

```
    /solu
```

```
        antype,trans
```

```
esel,all
```

```
nselect,all
```

```
timestep=1
```

```
time,timestep
```

```
solve
```

```
finish
```

! Saving the new interpolated field to quickly resume it afterwards

```
SAVE,Interpolation,db,,all
```

Interpolation Program

```
/prep7
```

```
*DIM,datanum1,,1
```

```
*VREAD,datanum1(1),out_xyzT_old,dat,,,,,,,,
```

```
(2x,F15.0)
```

```
nttold=datanum1(1)
```

```
*DIM,xyzTold,ARRAY,nttold,4
```

```
*VREAD,xyzTold(1,1),out_xyzT_old,dat,,JIK,4,nttold,,1
(2x,F12.8,2x,F12.8,2x,F12.8,2x,F12.8)
```

```
finish
```

```
/prep7
```

```
esel,s,mat,,201,203
```

```
nsle
```

```
*GET,nttnew,NODE,0,COUNT
```

```
*DIM,xyzTnew,ARRAY,nttnew,4
```

```
*GET,nmin,NODE,0,NUM,MIN
```

```
*do,I,1,nttnew
```

```
  *GET,Xcoor,node,nmin,LOC,x
```

```
  *GET,Ycoor,node,nmin,LOC,y
```

```
  *GET,Zcoor,node,nmin,LOC,z
```

```
  *VFILL,xyzTnew(I,1),DATA,Xcoor
```

```
  *VFILL,xyzTnew(I,2),DATA,Ycoor
```

```
  *VFILL,xyzTnew(I,3),DATA,Zcoor
```

```
  dxyzmin=1000.0
```

```
    *do,II,1,nttold
```

```
      dx=abs(Xcoor)-xyzTold(II,1)
```

```
      dz=Zcoor-xyzTold(II,3)
```

```
      dxyz=dx*dx+dz*dz
```

```
      *if,dxyz,lt,dxyzmin,then
```

```
        dxyzmin=dxyz
```

```
      *VFILL,xyzTnew(I,4),DATA,xyzTold(II,4)
```

```
    *endif
```



```

        *enddo
d,nmin,temp,xyzTnew(I,4)
*GET,nmin,NODE,nmin,NXTH
*enddo

/output,out_xyzT_new,dat

*VWRITE,nntnew
  (2x,F15.0)

*VWRITE,xyzTnew(1,1),xyzTnew(1,2),xyzTnew(1,3),xyzTnew(1,4)
  (2x,F12.8,2x,F12.8,2x,F12.8,2x,F12.8)

/output

finish

```

Solving Script

```

/clear

! Resuming the database containing the temperature field
interpolation, as well as model geometry, meshing, properties and
input data
resume,Interpolation,db

!File Renaming
/COPY,'WHHH','rth','','WHHHS','rth',''
/clear
/FILNAME,WHHHS,1

! Resuming the database containing mechanical constraints and
applied forces
resume,environment_stress,db

! Linear Buckling Analysis
! Mechanical pre-analysis
/assign,rst,WHHHS,rth
/solu
antype,stat
pstres,on

```

```
esel,s,mat,,201,203
nsle
ldread,temp,last,,,,WHHHS,rth
```

```
esel,all
nsel,all
```

```
solve
finish
```

! Eigenvalue Analysis

```
/solu
antype,buckle
bucopt,lanb,4
mxpand,4,,,yes
solve
finish
```

! Results saving

```
/COPY,'WHHHS','rth','','BUCK','rst',''
/FILNAME,BUCK,1
```

! Geometry Update

```
/PREP7
upgeom,0.01,,,BUCK,RST
finish
```

! Nonlinear Buckling Analysis

```
/solu
antype,static
nlgeom,on
!arclen,on
!nropt,full,,off
lnsrch,on
autots,on
pred,off
time,1
nsubst,10,,
rescontrol,define,all,1
outres,all,all
```

```
esel,all
nsle,all
```

```
solve
```

```
finish
```

Summary in italian

Questa tesi è stata svolta in collaborazione con l'ateneo di Hannover (Leibniz Universität) presso lo *Institut für Elektroprozessstechnik* (ETP). Lo scopo del lavoro è l'indagine e l'analisi del comportamento di una lastra metallica all'interno di un processo di riscaldamento per induzione a flusso trasverso. In particolare, l'attenzione è stata posta sul fenomeno di *buckling* termico che si verifica durante tale processo. Durante una prima fase, si è cercato di riprodurre il fenomeno tramite simulazione FEM; in seguito è stata effettuata un'analisi parametrica al fine di ricercare la possibilità di prevedere, controllare e/o limitare l'avvento del suddetto *buckling*. Per quanto concerne le simulazioni ad elementi finiti, il software che è stato utilizzato è ANSYS Mechanical APDL®.

La tesi si configura in cinque capitoli:

- Capitolo 1: nozioni preliminari;
- Capitolo 2: simulazioni multi-fisiche;
- Capitolo 3: il modello numerico;
- Capitolo 4: l'analisi parametrica;
- Conclusioni e prospettive.

Il primo capitolo riassume il lavoro di studio e comprensione del fenomeno del *buckling* termico nella fattispecie del processo studiato. Per quanto riguarda il riscaldamento per induzione a flusso trasverso è stata individuata, come più probabile causa del fenomeno, la distribuzione non omogenea della temperatura nella lastra riscaldata. Il metodo più diretto ed efficace per ottimizzare l'omogeneità di riscaldamento è la modifica del design dell'induttore utilizzato. Dal momento che la sostituzione di quest'ultimo non è stata possibile nel caso analizzato, il lavoro è proseguito nella direzione di studiare l'effetto, sull'entità del *buckling* e/o sulla sua presenza, della variazione degli altri parametri di processo.

Lo studio parametrico sopra citato è stato condotto tramite simulazioni ad elementi finiti multi-fisiche. Il secondo capitolo verte propriamente su questa tipologia di simulazioni numeriche e sugli strumenti adottati nel caso specifico. Il modello sviluppato utilizza come punto di partenza i risultati di una simulazione combinata (elettromagnetica e termica); il profilo termico di partenza viene letto ed interpolato e, successivamente, convertito in un campo di stress termici. A loro volta, quest'ultimi divengono la condizione iniziale dell'analisi strutturale di *buckling*.

I due principali strumenti per effettuare tale analisi messi a disposizione dal software ANSYS® sono: l'*Analisi lineare di buckling agli autovalori* e l'*Analisi non-lineare di buckling*. Un risultato della prima, che si rivelerà utile successivamente nello studio, è rappresentato dalla deformazione

qualitativa della lastra. I valori di sforzi e deformazioni prodotti dalla *Analisi non-lineare di buckling*, invece, hanno significato fisico. Questo tipo di analisi necessita, tuttavia, dell'introduzione di un'imperfezione nel modello affinché il fenomeno di buckling possa svilupparsi. L'imperfezione scelta a tal fine è stata la geometria deformata, generata dall'*Analisi lineare di buckling agli autovalori*. Questa deformazione viene utilizzata a meno di un fattore geometrico di scala per l'aggiornamento della geometria.

Il terzo capitolo illustra la procedura di costruzione del modello numerico in ogni sua parte. Sono inoltre riportati i frammenti di codici relativi ai singoli passi della costruzione, in modo particolare:

- Costruzione della geometria;
- Definizione degli attributi degli elementi della *mesh*;
- Definizione delle condizioni al contorno termiche (profilo di temperatura);
- Definizione delle condizioni al contorno strutturali (vincoli meccanici);
- Definizione e validazione della texture per il *meshing*;
- Definizione dei parametri indipendenti della simulazione: numero di modalità di buckling e fattore geometrico di scala per l'aggiornamento della geometria.

Il quarto capitolo contiene l'analisi parametrica, la quale rappresenta il nucleo centrale del lavoro di tesi. In questa sezione viene indagato l'effetto che la variazione di diversi parametri di processo ha sui risultati ottenuti. Nello specifico, è stata analizzata la variazione dei seguenti parametri fisici: lunghezza della lastra, forze applicate alla lastra, vincoli meccanici, proprietà dei materiali, temperatura applicata e spessore della lastra.

Nel complesso, i risultati ottenuti rispecchiano un comportamento fisicamente verosimile del modello sviluppato. Il codice scritto si candida quindi a diventare un utile strumento di analisi nell'ambito dello studio del fenomeno del *buckling* termico.

Come è riportato nel capitolo conclusivo (*Conclusioni e Prospettive*), i risultati del lavoro svolto devono essere inquadrati come un tassello all'interno di un mosaico più ampio che consta di un'analisi completa del processo di riscaldamento ad induzione. Questa analisi potrebbe essere condotta tramite una simulazione multi-fisica che copra gli ambiti elettromagnetico, termico e strutturale.

Un necessario futuro sviluppo di questo lavoro di tesi sarebbe la validazione sperimentale dei risultati ottenuti. Tale processo risulta essere, tuttavia, particolarmente complicato a causa delle difficoltà di misura di sforzi e/o deformazioni nel processo studiato. Difficoltà, quest'ultime, dovute alla stabilità del processo e alla temperatura di lavoro.